DISSERTATIONES
CHIMICAE
UNIVERSITATIS
TARTUENSIS
202

ASTRID DARNELL

Computational design of anion receptors and evaluation of host-guest binding

DISSERTATIONES CHIMICAE UNIVERSITATIS TARTUENSIS
202

DISSERTATIONES CHIMICAE UNIVERSITATIS TARTUENSIS
202

ASTRID DARNELL

Computational design of anion receptors and evaluation of host-guest binding

UNIVERSITY OF TARTU
Press

Institute of Chemistry, Faculty of Science and Technology, University of Tartu, Estonia

The dissertation is accepted for commencement of the degree of Doctor of Philosophy in Chemistry on 29.03.2021 by Council of Institute of Chemistry, University of Tartu

Supervisor:	Prof. Ivo Leito, PhD Institute of Chemistry, University of Tartu, Estonia
Opponent:	Prof. Dr. Katrina (Kate) Jolliffe The University of Sydney, Australia
Commencement:	May 20, 2021 at 10:15 Ravila Street 14a, Tartu (Chemicum)

Publication of this dissertation is granted by University of Tartu, Estonia.

This work has been partially supported by the Estonian Research Council grant PRG690. This work has been partially supported by Graduate School of Functional materials and technologies receiving funding from the European Regional Development Fund in University of Tartu, Estonia.

ISSN 1406-0299
ISBN 978-9949-03-590-8 (print)
ISBN 978-9949-03-591-5 (pdf)

University of Tartu Press
www.tyk.ee

TABLE OF CONTENTS

LIST OF ORIGINAL PUBLICATIONS

I. Tshepelevitsh, S.; Oss, M.; Pung, A.; Leito, I. Evaluating the COSMO-RS Method for Modeling Hydrogen Bonding in Solution. *ChemPhysChem* **2013**, *14*, 1909–1919.

II. Kadam, S. A.; Haav, K.; Toom, L.; Pung, A.; Mayeux, C.; Leito, I. Multidentate Anion Receptors for Binding Glyphosate Dianion: Structure and Affinity. *Eur. J. Org. Chem.* **2017**, *11*, 1396–1406.

III. Pung, A.; Leito, I. Predicting Relative Stability of Conformers in Solution with COSMO-RS. *J. Phys. Chem. A* **2017**, *121*, *36*, 6823–6829.

IV. Rüütel, A.; Yrjänä, V.; Kadam, S. A.; Saar, I.; Ilisson, M.; Darnell, A.; Haav, K.; Haljasorg, T.; Toom, L.; Bobacka, J. and Leito, I. Design, synthesis and application of carbazole macrocycles in anion sensors. *Beilstein. J. Org. Chem*. **2020,** *16*, 1901–1914.

V. Darnell, A.; Sikk, L.; Porosk, L.; Leito, I. Uncertainty of small enthalpy effects measured by isothermal calorimetric titration. *Journal of Chemical Metrology* **2021**,*15, 1*.

Author's contribution

Paper I: Part of the computational work (the computational study of 14 indolocarbazole-, pyrrole- and urea- based receptor molecules and estimation of 70 binding constants between small anions and the same receptor molecules), participated in writing the manuscript.

Paper II: All computational work (the computational study of 12 indolocarbazole- and urea based large receptor molecules and estimation of receptor-glyphosate binding constant values), participated in writing the manuscript.

Paper III: All computational work (the computational study of preferred conformations in solution for 105 small molecules), primary author of the manuscript.

Paper IV: All computational work – the computational study of 15 receptor molecules and their complexes with 5 anions (a total of 75 complexes and 15 free receptors), participated in writing the manuscript.

Paper V: All Experimental work, application of the component-by-component approach (realized via the Kragten method) for the uncertainty estimation of ITC experiments, primary author of the manuscript.

ABBREVIATIONS

BP	Becke-Perdew, a class of DFT functionals
Calc	Computationally determined values
COSMO-RS	Conductor-like Screening MOdel for Real Solvents
CSM	Continuum solvation model
DFT	Density functional theory
DMSO	Dimethyl sulfoxide
Exp	Experimentally determined values
ΔG	Reaction free energy
ΔH	Reaction enthalpy
HB	Hydrogen bond
HBA	Hydrogen bond acceptor
HBD	Hydrogen bond donor
IC	Indolocarbazole
IMHB	Intramolecular hydrogen bond
ITC	Isothermal titration calorimetry
ISE	Ion selective electrode
K_{ass}	Association constant of a host-guest complexation reaction
MD	Molecular dynamics
NMR	Nuclear magnetic resonance spectroscopy
OCE	Outlying charge error
SMD	Solvation Model based on Density
TZVP	Valence triple-zeta polarization (basis set)
TZVPD	Valence triple-zeta polarization with diffuse functions (basis set)
UV/Vis	Ultraviolet-visible

INTRODUCTION

The field of supramolecular chemistry and its subfield – host-guest binding of ions by receptor molecules – have undergone rapid growth in the past few decades. Many different receptor molecules have been designed, synthesized and investigated by a large number of research groups for the binding of molecules and ions.[1] Receptor molecules are finding applications in a number of fields, for example safety screening and environmental protection, pharmaceutical industry (drug formulation and delivery) and biomedical analysis.[2–5] Anion receptor chemistry has found applications in catalysis, extraction of components in samples and as a drug transport system for medicine.[1] Receptors and receptor array systems are studied with a purpose to create easily portable analysis devices that could determine analyte content from the studied samples with on-site real-time analysis.[6]

The host-guest complex formation occurs through the combination of several effects, e.g. hydrogen bond formation (commonly the strongest interaction contributing to complex formation), hydrophobic interactions, sigma hole interactions (electrostatic interaction between the electron-rich parts of the anion and the electron-poor areas in the receptor molecule), steric effects etc.[7–10] There are a number of principles that should be accounted for in receptor design: preorganization (free host compound should have similar geometry to the host-guest complex), cooperativity (multiple binding sites of a receptor can interact with each other to enhance binding), complementarity (the geometry of the binding sites/cavity size of a receptor should match the size and geometry of the guest species).[11]

The goal of this work was to study the possibility of investigating anion-receptor binding in order to help design receptors for a selection of analytically important anions, using the COSMO-RS computational method. Emphasis is put on the investigation of steric effects and the fit of the receptor and anion geometries and their role in receptor-guest binding, as well as probing the limits of COSMO-RS in predicting the different aspects of receptor-anion binding (geometry, steric effects, strength of binding). The wider purpose of thoroughly investigating these effects and the possibilities of their prediction is to construct more selective receptors with a higher binding affinity in the future.

The investigations were carried out in the following parts.

In work [III], the ability of COSMO-RS approach to correctly predict conformer stability in solutions was tested by studying 105 small molecules, which have experimental information about the relative stability of their conformers in different solvent environments published in past studies. The goal of this part of the work was to determine whether COSMO-RS can accurately predict the most stable conformers of molecules in the chosen solvent environment.

In work [I], the binding affinities of small indolocarbazole- and urea-based receptors towards small monoanions were computationally estimated and the predictions compared with experimental data found from literature. Depending

on the availability of previously published experimental data for the respective receptor molecules, the following anions were studied: F^-, Cl^-, Br^-, I^-, HSO_4^-, $PhCOO^-$, $H_2PO_4^-$, NO_2^-, NO_3^-, TsO^-. The aim of work [I] was to check whether COSMO-RS can predict the binding affinities (characterized by the association constants of the binding reactions) for receptor-anion complexation and predict the trends in binding strength when comparing different receptor molecules or different anions.

In work [II], 12 large anion receptor molecules based on indolocarbazole-, urea- and biscarbazolyl groups used as binding fragments were investigated for their binding affinities toward the glyphosate dianion. This allowed to additionally test the suitability of the computational method as all experimental results for this group of molecules have been measured using a consistent methodology and all-important experimental parameters (e.g. the water content of the used solvents) are accurately known. Studying similar receptor molecules together will also give better understanding on how the binding affinity depends on the structure of a receptor molecule. The study investigated the effects of receptor structure on the binding affinity for the glyphosate dianion. The purpose is to find out, how the length and rigidity of the receptor structure between the binding sites affects the complex formation and to investigate the resulting steric effects and their relationship towards the receptor-anion binding affinity.

In work [IV], a set of macrocyclic anion receptors were researched. Macrocyclic receptors often have higher binding affinities; their selectivity may be more easily tunable and the preorganization effect of the receptor can be achieved more easily. The goal of the computational part of work [IV] was to study the effects of macrocycle geometries, structural rigidity and cavity size on the binding of a number of carboxylate anions, to find, whether clear trends in binding affinity can be identified and tied to the construction of the receptor.

The second part of the study (work [V]) investigates the applicability of isothermal titration calorimetry (ITC) for measuring the thermodynamic parameters – K_{ass}, ΔH – of a binding reaction with low K_{ass} and ΔH values. Low K_{ass} and ΔH values are very common in supramolecular chemistry. This work was carried out on the basis of a well-known model reaction – the complexation of K^+ with 18-crown-6. The results of the experimental study were compared with data from a number of literature sources. A thorough uncertainty estimation was carried out to estimate the accuracy of the experimental predictions and the uncertainty budget analyzed to determine the dominant contributors to the measurement uncertainty.

1. LITERATURE OVERVIEW

1.1 Supramolecular chemistry

Supramolecular chemistry as a field is defined as the study of intermolecular interactions and binding between molecules, ions and their aggregates through interactions other than covalent bond formation. The field involves studies of host-guest complex formation and the behavior of macromolecular systems and investigates the extent and characterization of different contributors to binding strength in various biological or synthetic systems.[12,13]

In host-guest chemistry, a receptor is defined as a molecule that can be used for detecting the presence of quantity of another molecule or ion from a solution.[11] Interaction between the receptor molecule (the host) and the studied analyte (the guest) causes a measurable change in the solution properties, which is then measured to determine the existence or quantity of the studied guest.[13] Many different types of interactions can occur simultaneously to achieve complexation. These interactions include hydrogen bonding, ion pair formation, hydrophobic effect and electrostatic interactions. A number of detection methods are used in anion receptor chemistry, for example fluorescence spectroscopy, UV/Vis spectroscopy, potentiometry or even naked eye detection.[6,14–16]

Selectivity is a very important parameter for the use of receptor molecules. Typically, a single receptor molecule is not fully selective to one guest, but can bind a number of chemical species with different binding affinities.[17] As the binding affinity of a receptor towards a specific guest depends on a number of different interactions occurring simultaneously, both the selectivity of a receptor towards a specific guest and the binding affinity values of receptor-guest complex formation tend to not be straightforward to predict.[18]

As a way to solve the issue of low receptor selectivity, research is carried out about the possibility of using receptor arrays for the simultaneous investigation of the behavior of a number of receptor molecules with the same analyte, in order to attempt to obtain a selective result from the behavior of the array.[19]

1.2 Anion receptors

As most of this study focuses on anion receptors, the literature overview also centers the focus on the binding interactions and previous literature studies of these receptors. A large variety of molecules have been studied in the past to try to find suitable receptor molecules for the detection of various anions.[1] Some examples of small receptors that primarily bind anions through hydrogen bonding interactions include molecules containing pyrrole, indole, indolocarbazole, urea and thiourea groups.[20–24]

1.3 Types of binding interactions in anion-receptor complex formation

In anion receptor chemistry, a number of different interactions can occur between the host molecule and the guest that influence the binding affinity.

Many receptor molecules mainly interact through hydrogen bonding – the interaction between a hydrogen bond donor (HBD) group in one species (the receptor) and the hydrogen bond acceptor (HBA) group of the other (the anion). Hydrogen bonds are highly directional and the strength of the interaction largely depends on the bond angle (the typical characteristics are 175–180° bond angle for strong hydrogen bond interactions, 130–180° for medium strength hydrogen bond interactions and 90–180° for weak hydrogen bond interactions) [25] and the distance between the atoms involved in the interaction (the distance of HBD and HBA groups is between 1.2...2 Å),[25] which makes studying the preferred conformations of both the free host molecule and the host-guest complex very important. As the strength of the hydrogen bond interaction also strongly depends on the partial charges on the respective HBD and HBA fragments (higher partial charges enhance the strength of the HB), ions tend to form stronger interactions than neutral species.[25]

Anion receptors are often designed to have multiple HBD sites, which will improve the binding strength, as long as the receptor-anion complex geometry enables a suitable arrangement of the binding groups for strong HB interactions. A receptor may be designed to contain both HBD and HBA sites for the purpose of stabilizing the preferred receptor conformation to a specific spatial arrangement through the formation of intramolecular HBs.[10]

Solvent effects are important to account for as the number of solvent molecules is very large in solutions compared to the small concentrations of receptor and anion. When complex formation requires the removal of a solvation layer of solvent molecules, binding becomes energetically less favorable.[8,26] Hydration of species in solutions plays an important role in binding in water, but even when non-aqueous solvents are used, the HBD ability of the solvent or small water content in the solvent will influence the strength of host-guest binding. The HBA ability of the solvent is also very important, as in such environment the solvent molecules will be able to interact with the HBD groups of the receptor and compete with the anions in complex formation.[7]

Hydrophobic (or more generally, solvophobic) interactions can also have an important role in improving the binding affinity for anion receptors.[27] For example, in solvent environments with a high water content, hydrophobic binding pockets may improve the binding abilities of a host compound towards anions that have a large hydrocarbon moiety in their structure.[28] Receptor molecule designs have been investigated that specifically focus on binding partially hydrated anions into hydrophobic receptor cavities.[29,30] Additionally, the hydrophobic interactions can help with the preorganization of the receptor structure and can assist in the binding between certain hosts and guests.[31] Hydrophobic

interactions can be used to assist on enhancing the receptor selectivity towards specific anions based on their hydrophilicity.[32]

In some systems, ion pair formation assists in complex formation.[33] Electron-rich host molecules have been designed to bind electron-deficient guests.[34]

1.4 Effects on complexation

In supramolecular chemistry, a number of effects are discussed when characterizing receptor molecules and their binding properties.[11,13]

Co-operativity effects – simultaneous interactions of different binding sites of a receptor molecule with the bound guest – may improve the strength and selectivity of binding.[35]

A large number of past studies focus on the „lock-and-key" principle – the focus on the importance of exact geometrical matching for the receptor and guest. According to the principle, receptors should be designed in a way that the geometries of receptor and guest would achieve a perfect fit with one another by both size and the spatial arrangement of binding groups and anionic center(s). However, more recent studies advise that this reasoning may be insufficient to predict successful binding.[36] For example, in the case of macrocyclic receptors with internal cavities, the role of „high-energy" water in the receptor cavity has been found to play a vital role in the binding interactions.[26]

Complementarity and preorganization – the principles that the spatial arrangement of the receptor's binding sites should be suitable for the bound guest and that the free receptor should have a preferred geometry similar to that of the bound complex – help achieve higher binding affinities. These principles help guarantee that complex formation is not energetically unfavorable due to large-scale reorganization of the receptor structure.[13,37]

1.5 Experimental characterization and studies of binding

Experimental determination of the association (binding) constant K_{ass} of the host-guest binding reaction can be carried out by a many methods (e.g. UV/Vis spectroscopy, NMR spectroscopy, fluorescence spectroscopy, potentiometry etc.), depending on the properties of the studied receptor and guest.[38]

The 1:1 complex formation between receptor R and anionic guest A^- can be expressed by equation (1):

$$\mathrm{R} + \mathrm{A}^- \underset{}{\overset{K_{ass}}{\rightleftharpoons}} \mathrm{RA}^- \qquad (1)$$

The association constant K_{ass} for the reaction is found according to equation (2), where a are the activities of the respective species:

$$K_{\mathrm{ass}} = \frac{a(\mathrm{RA^-})}{a(\mathrm{R})\cdot a(\mathrm{A^-})} \tag{2}$$

The reaction standard free energy ΔG is expressed via the free energies of the respective species in solution by equation (3):

$$\Delta G = G(\mathrm{RA^-}) - G(\mathrm{R}) - G(\mathrm{A^-}) \tag{3}$$

The reaction standard free energy ΔG and the association constant K_{ass} are related according to equation (4):

$$\Delta G = -RT\ln K_{\mathrm{ass}} \tag{4}$$

Determining the reaction enthalpy and entropy is more difficult than determining the association constant of a binding reaction. The study of reaction enthalpy ΔH is carried out with isothermal titration calorimetry (ITC) or the use of the van't Hoff method. The van't Hoff method is based on multitemperature determination of association constant values and the construction of the van't Hoff curve ($\ln K$ vs $1/T$) for the determination of thermodynamic parameters of the reaction (the $\ln K$ values can be determined with ITC or another experimental method). Calorimetric determination may be limited by access to a suitable calorimeter, low solubility or availability of the receptor or guest compound, inaccuracies in experimental determination of heat effects for low affinity binding reactions etc.[39,40] The van't Hoff method is commonly considered less accurate than ITC.[41–46] Various explanations have been suggested for the discrepancies between the results determined by van't Hoff and ITC approaches. Some of the possible causes include the possibility of other, hard to quantify temperature-dependent interactions simultaneously occurring in the studied system (which affect the van't Hoff approach but not direct ITC determination); inaccuracies in the mathematical models used for the data treatment or other measurement uncertainty sources.[41–46]

For studying low binding affinity systems with ITC experiments, the choice of suitable experimental parameters is very important. A very common method for the data treatment of ITC experiments is based on the Wiseman isotherm, the shape of which can be characterized by the Wiseman „c" parameter.[47] This parameter is calculated from the reaction stoichiometry coefficient n, the receptor cell concentration M_{t} and the association constant K_{ass} according to equation (5):

$$c = \mathrm{n}M_{\mathrm{t}}K_{\mathrm{ass}} \tag{5}$$

Ideally, the „c" parameter value should be between 5(10) and 100 (different sources quote different values).[47–49] With low „c" parameter values ($c < 1$), the shape of the titration curve loses some defining characteristics and finding the reaction parameters from the curve will be associated with higher uncertainty.

Some past studies have suggested that with careful experimental planning, low „*c*“ value experiments („*c*“ value between 0.01–1) can be used to obtain sufficiently accurate results, when certain requirements are met.[40,50,51] Ideally, experiments should be planned so that the majority of receptor has been bound to complex by the end of the titration.[50] This can be difficult to achieve for low binding affinity systems as the solubility or usable maximum concentrations of the receptor or guest may be limited and thus it is not always possible to achieve a „*c*“ value above 1 and near-complete receptor complexation at the end of the experiment.

1.6 Computational studies of binding

The binding affinities can be expressed by association constant K_{ass} values, which are calculated from the computational estimates of free energies of the receptor, guest and receptor-guest complex in the chosen solvent environment (equations (3) and (4)). While computational studies of chemical species under vacuum (gas phase) conditions can generally make quite accurate predictions, carrying out computational investigations in solutions is more complex.

There are a number of reasons why computing the equilibrium of anion-receptor binding (i.e. binding affinity) in solution is not a simple computational task.[38,52] In a solvent environment, a large variety of constantly changing interactions with other molecules and ions (solvent molecules, impurities, molecules of the compounds of interest) take place that affect the behavior of a chemical species. As a result, the modelling of solvent behavior is complex and computationally resource intensive.

Some computational approaches (e.g. molecular dynamics simulations) either use a high level of simplification in the approach or have a very high computational resource cost, which can be a limiting factor in their application.[53] In order to make the computational resource costs feasible for practical applications, often semi-empirical methods (the computations are simplified, and some approximations are made in the computational approach based on experimental data) are applied for the modelling of solvent environments. The choice of a method to use can be limited by the choice of solvent – certain computational methods (e.g. continuum solvation models such as the widely used SMD approach) are parametrized with the physical parameters of the used solvent environments and may not be applicable to all solvent environments.[54]

Correct computational predictions require the correct estimation of all interactions that may influence binding. Accurately computationally describing solvent effects, HB interactions, coordinative effects and certain long-range interactions can be difficult. The study of anionic species and their interactions is more difficult than the study of neutral molecules as the increased charge densities will affect the interactions between different species in the solvent environment and may multiply or introduce new errors to the predictions.[38,55] For example, one computational error that is more prominent in the study of anions

is the outlying charge error (OCE). It is caused by a part of the electron density being allocated outside the molecular cavity during the computations, which causes misestimation of the molecular charge and local electron densities.[56]

One computational method with a number of useful characteristics is COSMO-RS (COnductor-like Screening MOdel for Real Solvents).[57] The working principle of the COSMO-RS computational method involves two steps.

The first step of the method is a modification of continuum solvation models (CSMs). This step applies the dispersion-corrected density functional theory (DFT) approach on molecules in an ideal conductor (the model assumes that the molecules are suspended in a conductor environment of $\varepsilon = \infty$). From the calculations, the total energy, electron density and polarization charge densities on the surface of the studied molecule are predicted in a virtual conductor. This step also yields the optimized molecular geometry.[57]

The second step takes into account interactions between real molecules, by studying pairwise interactions of charged molecular surface segments. The aim of the step-by-step simulation of pairwise molecular contacts is to move from a system where the molecules are separate and placed in a virtual conductor, to a system resembling the closely packed liquid environment.[57]

In the COSMO-RS approach, for characterizing the interactions between the chemical species in the solution, all species (solute molecules, solvent molecules, any impurities) are treated similarly. All types of interactions (hydrogen bonding, van der Waals forces, electrostatic interactions etc.) are taken into account between all species in the solution.[57]

The strengths/advantages of the COSMO-RS computational method are (1) the ability to study multicomponent solutions with a large variance in compound concentrations (i.e. not limited to dilute solutions), (2) the possibility to account for temperature effects, (3) that parametrization of the method is not fixed to any specific solvent (i.e. any molecules can be used as solvent molecules) and (4) that the calculation is computationally highly efficient.[58] This means that multicomponent solutions can be studied with the method, which is very important as this is very commonly the case for experimental studies conducted on anion-receptor binding.[59,60] In addition, a correction factor for OCE (a common computational error especially prominent in the study of anions) is applied in COSMO(-RS) approach and the COSMO algorithm is considered to be less sensitive to OCEs than some other continuum solvation models.[56,61]

The advantages 1 and 3 are important in comparison with a number of solvation methods that enable computations only in infinitely dilute solutions in predefined solvents, such as the widely used SMD approach.[54] A 2015 summary paper considers COSMO(-RS) a reliable method with which high overall accuracy is achievable for the study of chemical potentials of molecules in solvent environments.[62] On the other hand, advantage 4 makes COSMO-RS usable for large molecules, differently from some really high computational quality methods, such as *ab initio* molecular dynamics.[63]

The weaknesses of the method are extensive parametrization and the use of a simplified approach to account for intermolecular interactions. Moreover, the parametrization is updated regularly and thus, the results of COSMO-RS computations differ depending on which parametrization was used. While there can be notable changes in the absolute values of the predictions, relative values remain similar between different parametrizations (as also demonstrated below).[64] As the method describes intermolecular interactions through the pairwise interactions of surface segments of the interacting species, some of the steric effects of molecular interactions may be not accounted for completely and the method is unable to account for some long-range interactions between molecules.[61,65] It has also been suggested that the method may have problems with describing long-range sterically dependent interactions that are strongly affected by solvation. This can cause problems in the study of systems with multiple inter- and intramolecular hydrogen bond interactions – when numerous interactions occur simultaneously between different parts of two chemical species or when the existence of one HB depends on the existence or lack of another HB interaction, this can be difficult to computationally predict.[65]

On the basis of the balance of the above listed strengths and weaknesses, the COSMO-RS computational method was chosen for this work.

2. EXPERIMENTS AND COMPUTATIONS

2.1 Computational parameters

The DFT calculations were carried out using the program Turbomole v.6.2 (work [I]), v.6.4 (work [II]), v 6.5 (work [III] and work [IV]).[66–69] Geometry optimization was carried out using the Becke-Perdew functional.[70,71] The following parameters were used: TZVP (triple zeta valence with polarization functions) basis set, wave function convergence criteria: max difference 10^{-6} Hartree, geometry convergence: max gradient |dE/dxyz| 10^{-3} Hartree $Bohr^{-1}$.

For studying the applicability of the COSMO-RS method for the prediction of most stable conformers of small molecules (work [III]), stricter criteria were applied: Becke-Perdew functional, TZVP basis set, wave function convergence criteria: max difference 10^{-7} Hartree, geometry convergence: max gradient |dE/dxyz| 10^{-4} Hartree $Bohr^{-1}$.

The initial geometries were chosen by estimating the possible geometric orientation of the flexible groups in the molecule and investigating how the different flexible parts of the molecule could be oriented towards one another. A large number of initial geometries (up to around 20 for the more complex structures) were given to the computational software as input for the DFT calculations and geometry optimization. As no limits were set for the movement of atoms during the geometry optimization, at times, the optimized geometries were often quite different from the initial starting geometries. The optimized geometries were then studied to find and omit duplicates of very similar (essentially identical) geometries and the set of obtained unique conformers used for the COSMO-RS calculations. It must be noted that while the initial treatment of conformers studied a large number of geometries, commonly the COSMO-RS approach estimates that only 1–3 of the most stable conformers exist in the solvent environment. However, it is vital that these most stable conformers have been found and submitted to the program for the computational predictions to be accurate. For this reason, a thorough investigation into possible conformers is very important. The handling of conformers in the COSMO-RS approach using COSMOtherm is described in work [III].

For works [I] to [IV], the newest (at that time) version of the program COSMOtherm was used with the following parametrizations: BP_TZVP_C30_1201 in work [I]; BP_TZVP_C30_1401 in work [II]; BP_TZVP_C30_1701 in work [III]; BP_TZVP_C19 in work [IV].

For work [III], all calculations were also carried out at the BP_TZVPD_FINE computational level to test whether the predictions remain the same. Overall, large differences were not noted, except for the case of one molecule, where the order of conformer stability was in fact predicted incorrectly by BP_TZVPD_FINE. Thus, the BP_TZVP was found suitable for the study of small molecules.

A 2011 study that investigated the effects of using different basis sets in the COSMO-RS method for the calculation of affinity coefficients noted that at least valence double-beta basis set is necessary but using larger basis sets did not show advantages.[72]

2.2 Experimental parameters

ITC measurements were carried out with a MicroCal iTC_{200} unit at the University of Tartu Institute of Technology. The full experimental details are presented in work [V] and its SI. A brief description is provided here. All experiments were conducted at 298 K. 200.6 µl of 18-crown-6-ether solution with the concentration of 0.005M of was loaded into the calorimetric cell and KCl solutions of 0.1 to 0.05 M were added in 19 steps of 2 µl during the titration. An initial injection of 0.2 µl was made to account for the effects of diffusion of titrant into the cell during initial thermal equilibration and the corresponding data point later removed prior to data analysis. Separate experiments were carried out to account for the effects of heat of dilution and the determined heats of dilution were subtracted from the titration experiment prior to data treatment. Data treatment was carried out using MS Excel and a Python script. The Python script used for this work was originally created by Dr Lauri Sikk. The present author later modified and tested different mathematical models for determining the active concentrations and heat effects.

The scheme of the typical ITC experiment is presented at Scheme 1. [V, SI]

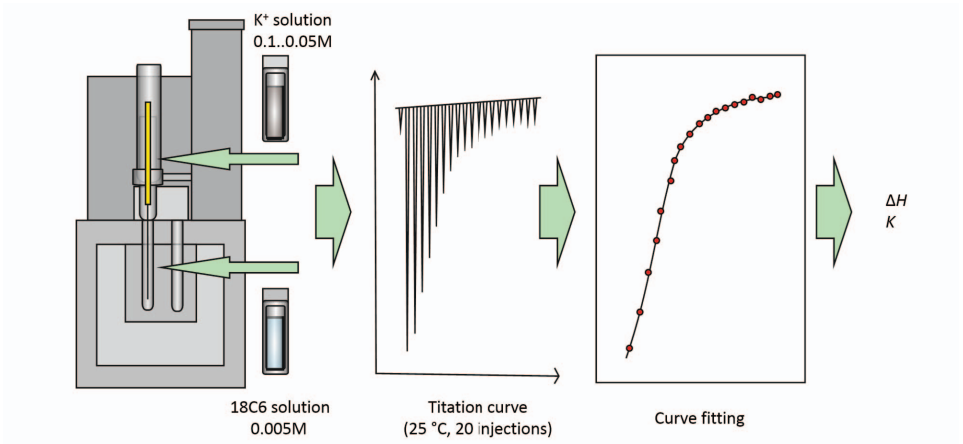

Scheme 1. ITC titration experiment.

MicroCal iTC$_{200}$ is a perfusion instrument and uses the following approach to treat the estimation of volume and concentration effects and the calculation of total heat effects of the studied reaction:

- The instrument uses a preset „active volume“. The heat effects of reaction happening inside the active volume are fully visible for the instrument. For the MicroCal iTC$_{200}$ instrument, the active volume V_0 = 200.6 µl.
- During the experiment, at each injection, a set volume is injected to the active volume of the instrument and the same amount of the solution of the composition after the previous injection is pushed out into the overflow area above the calorimetric cell compartment.
- The total heat effect is calculated from equation (6), where Q_{tot} is the total heat effect of the binding reaction, n is the reaction stoichiometry, M_t is the active concentration of the cell compound, ΔH is the reaction enthalpy, V_0 is the active volume, X_t is the active concentration of titrant, and K_{ass} is the association constant of the binding reaction.[73]

$$Q_{\mathrm{tot}} = \frac{nM_{\mathrm{t}}\Delta HV_0}{2}\left[1 + \frac{X_{\mathrm{t}}}{nM_{\mathrm{t}}} + \frac{1}{nK_{\mathrm{ass}}M_{\mathrm{t}}} - \sqrt{\left(1 + \frac{X_{\mathrm{t}}}{nM_{\mathrm{t}}} + \frac{1}{nK_{\mathrm{ass}}M_{\mathrm{t}}}\right)^2 - \frac{4X_{\mathrm{t}}}{nM_{\mathrm{t}}}}\right] \quad (6)$$

- However, as the solution in the overflow compartment also has a small effect on the measurable heat, equation (7) is used to account for this. The middle term of the equation characterizes the effect of the solution in the overflow area. In equation (7), v_i is the volume of injection i, V_0 is the active volume of the instrument and Q(i) is the uncorrected total measurable heat up to injection i.[73]

$$\Delta Q(\mathrm{i}) = Q(\mathrm{i}) + \frac{v_{\mathrm{i}}}{V_0}\left[\frac{Q(\mathrm{i}) + Q(\mathrm{i}-1)}{2}\right] - Q(\mathrm{i}-1) \quad (7)$$

- In order to estimate the active concentrations of the receptor and cation during the experiment, equations (8) and (9) are used. X_{t0} and M_{t0} are the initial concentrations of compounds in the calorimeter cell (host) and the syringe (guest), $V_{tot\ i}$ is the total injection volume at the current point of the experiment and V_0 is the active volume of the instrument. Equation (10) is used to calculate the initial guest concentration Xt_0 from initial solution concentration in the syringe $c_{syr.}$[73]

$$M_{\mathrm{t}} = M_{\mathrm{t0}}\left[\frac{1 - \frac{V\mathrm{tot_i}}{2V_0}}{1 + \frac{V\mathrm{tot_i}}{2V_0}}\right] \quad (8)$$

$$X_{\mathrm{t}} = X_{\mathrm{t0}}\left[\frac{1}{1 + \frac{V\mathrm{tot_i}}{2V_0}}\right] \quad (9)$$

$$X_{\mathrm{t0}} = c_{\mathrm{syr}}\left[\frac{V\mathrm{tot_i}}{V_0}\right] \quad (10)$$

3. RESULTS AND DISCUSSION

I Computational study of anion-receptor binding

3.1 Studying the usability of the COSMO-RS method

3.1.1 Studying small molecules and anions with COSMO-RS

In order to start computational investigation of receptor-anion binding, the suitability of the COSMO-RS method for this purpose (studying complex geometries, correctly estimating the most stable conformers in a chosen solvent environment, computationally estimating the binding strength between receptors and anions) was tested.

In work [I], simple indolocarbazole-, pyrrole- and urea- based receptor molecules were studied for binding small monoanions (e.g. Cl^-, F^-, Br^-, HSO_4^-, $H_2PO_4^-$ and $PhCOO^-$). The most stable conformers were determined, and the geometries of the complexes studied by COSMO-RS. The computational estimates for the free energies were determined for the anion, free receptor and the receptor-anion complex in the chosen solvent environment and equations (3) and (4) were used to find the computational estimates of binding constant values, which were then compared to previously published experimental results from a number of research groups.[17,22,23,74–77]

Table 1 presents the comparison of the computational predictions obtained by the COSMO-RS approach and the experimental $\log K_{ass}$ values taken from ref. 22.

Table 1. Experimental and computationally predicted logK_{ass} values for 4 small receptor molecules binding small monoanions (Parametrization: BP_TZVP_C30_1201). Experimental data from ref. 22. The values for RM1 are presented as absolute values, for RM2-RM4, relative values compared to receptor RM1 are presented.

Solvent: Acetone, 50ppm H_2O[a]		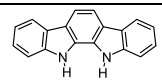 RM1	Relative logK_{ass} values[b]	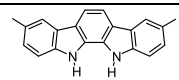 RM2	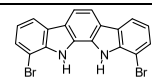 RM3	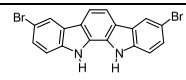 RM4
F^-	logK_{ass}, calc	24.0	Δ, calc	-0.3	1.3	1.0
	logK_{ass}, exp	4.7	Δ, exp	0.0	-1.1	1.0
Cl^-	logK_{ass}, calc	8.1	Δ, calc	-0.2	-0.5	0.3
	logK_{ass}, exp	4.5	Δ, exp	-0.4	-0.5	0.3
$PhCOO^-$	logK_{ass}, calc	11.5	Δ, calc	-0.2	-2.7	0.7
	logK_{ass}, exp	5.3	Δ, exp	0.1	-0.9	0.6
$H_2PO_4^-$	logK_{ass}, calc	10.3	Δ, calc	-0.2	-4.2	0.7
	logK_{ass}, exp	4.9	Δ, exp	0.3	-0.8	0.4
HSO_4^-	logK_{ass}, calc	5.2	Δ, calc	-0.3	-2.7	0.3
	logK_{ass}, exp	low[c]	Δ, exp	low[c]	low[c]	low[c]

[a] Experimental solvent water content is estimated for the calculations as the precise value was not presented in ref. 22.

[b] The logK_{ass} values for RM2 to RM4 are given as relative values compared to RM1 (Δ,X = logK_{ass}, X – logK_{ass}, RM1). For RM1, the absolute logK_{ass} values are presented.

[c] According to ref. 22, the logK_{ass} values for HSO_4^- complexes were too low for accurate experimental determination.

The results in Table 1 show that the COSMO-RS method cannot be used to satisfactorily predict the *absolute values* of binding constants for anion-receptor binding. All investigated binding constant values are overestimated by a large margin, but an extreme discrepancy between experimental values and computational predictions occurs for F^- complexes. This could be attributed to the properties of the fluoride anion and the limitations of the COSMO-RS method in predicting the behavior of small anions with a highly localized charge.[57] Similar results to those presented in Table 1 were observed for predicting the binding for other receptor molecules studied in work [I].

When looking at the ability of the COSMO-RS method to predict *trends in binding* (whether one receptor binds one anion better than the others, or whether one anion is bound better by one receptor than the others), these trends are largely reproduced in the computational predictions. However, this was not the case for every anion, especially not in the case of the F^- anion.

The results of work [I] indicate that while COSMO-RS cannot accurately predict the absolute values of binding constants of anion-receptor binding, it can make some tentative predictions about the trends occurring in binding when comparing a number of receptors or guests.

After investigating the geometries of the studied small receptor molecules, urea-, indole-, carbazole- and indolocarbazole fragments were chosen as suitable building blocks for receptor candidates for further study in anion receptor design.

3.1.2 The effects of parametrization choice and the estimation of solvent water content to the computational predictions

The input parameters used for the application of the COSMO-RS method may influence the obtained computational predictions. Two important parameters are choosing the parametrization that is used by the program and applying accurate estimation of water content to the nonaqueous solvent environment used in the calculations. As the conclusions of work [I] determine that the absolute binding constant values are highly overestimated, it was checked that these misestimations are not caused by the choice of a specific COSMO-RS parametrization or by the misestimation of water content in the studied solvent environment.

Table 2. The effect of parametrization choice on the computational predictions of logK_{ass} values for indolocarbazole (RM1)-anion complexes.[a]

Year of release of the respective BP_TZVP level parametrization[b]											
Acetone,50 ppm H_2O	2010	2011	2012	2013	2014	2015	2016	2017	2018	2019	2020
$\Delta\log K_{ass}$, $PhCOO^-$	3.4	3.4	3.4	3.5	3.4	3.4	3.4	3.5	4.2	4.2	4.2
$\Delta\log K_{ass}$, F^-	15.5	10.5	15.9	17.1	16.8	16.6	16.6	16.7	16.7	16.5	16.5
$\Delta\log K_{ass}$, $H_2PO_4^-$	2.3	2.0	2.2	2.2	2.1	2.2	2.0	2.0	2.6	2.7	2.7
$\Delta\log K_{ass}$, HSO_4^-	-2.9	-3.2	-2.9	-3.1	-3.1	-3.1	-3.1	-3.1	-2.5	-2.5	-2.5
$\log K_{ass}$, Cl^-	8.0	9.4	8.1	8.0	8.3	8.4	8.4	8.6	12.7	12.9	12.9

[a] The $\Delta\log K_{ass}$, X values are presented for all ions except Cl^- and are expressed relative to Cl^- ($\Delta\log K_{ass}$, X = $\log K_{ass}$, X – $\log K_{ass}$, Cl^-). For Cl^- absolute $\log K_{ass}$ values are presented.

[b] In 2011, a special parametrization for better accounting for HB interactions was released. The 2011 results in this table are calculated using this special parametrization, BP_TZVP_C21_0111_HB_2010.

From Table 2, it can be seen that no matter which parametrization is chosen, the predictions of absolute values of the binding constants differ greatly from the experimental values (Table 1), as well as (although to a lesser extent) between parametrizations, but at the same time, the relative changes are similar, which indicates that the choice of parametrization does not have a notable effect on changing the accuracy of the predictions, as all the predictions are highly approximate in any case. In 2011, a special parametrization was released to improve the predictions for hydrogen bond interactions. While the use of this parametrization lowers the overestimation of F^- binding affinity slightly, it does not improve the accuracy of other predictions. In 2018, some changes were made in the COSMO-RS method related to the base parameters used to estimate the chemical potential of compounds in the solvent environment.[78] From that year on, computational predictions of anion-receptor binding constant values yield $\log K_{ass}$ values increased by around 4–5 $\log K$ units (the misestimation of absolute binding constants increased), but the relative differences (the trends in the predictions) remain similar.

From 2012–2020, COSMO-RS allows to use a computational level improved from BP_TZVP: BP_TZVPD_FINE. The binding affinity of RM1 and Cl^- was studied with this computational level and the respective yearly parametrizations, the results are shown in Table 3.

Table 3. Comparison of using BP_TZVP and BP_TZVPD_FINE computational levels for the prediction of $\log K_{ass}$ values for indolocarbazole (RM1)-Cl^- complex.[a]

Solvent: Acetone, 50 ppm H_2O	2012	2013	2014	2015	2016	2017	2018	2019	2020
$\log K_{ass}$; BP_TZVP	8.1	8.0	8.3	8.4	8.4	8.6	12.7	12.9	12.9
$\log K_{ass}$; P_TZVPD_FINE	6.1	5.7	6.7	6.5	6.2	8.0	11.8	15.9	15.9

[a] $\log K_{ass}\_exp = 4.5$[22]

It can be seen from Table 3 that while the predicted binding constant values are different for BP_TZVP and BP_TZVPD_FINE, neither computational level yields accurate predictions for the absolute binding constant values. The larger overestimation occurring from 2018 onwards for the BP_TZVP computational level also occurs in the BP_TZVPD_FINE level. As using the BP_TZVPD_FINE computational level takes more computational resources, but it does not yield higher accuracy of the predictions, the computations in future work were carried out using the BP_TZVP computational level.

It is also vital to correctly account for the water content in non-aqueous solvents, as even low water content in the solvent can strongly influence the strength of receptor-anion binding. Table 4 shows the effect of water content of acetone solvent on the computational binding constant estimates for the anion complexes of receptor RM1 (Parametrization: BP_TZVP_C30_1201).

Table 4. The effect of solvent water content on anion binding by receptor RM1.

Solvent: Acetone	Computational logK_{ass} values at different water contents:					Exp. logK_{ass} values[22]
	0 ppm	50 ppm	500 ppm	5000 ppm	50000 ppm	(water content unknown)
logK_{ass}, $PhCOO^-$	11.6	11.5	11.1	9.7	6.7	5.3
logK_{ass}, Cl^-	8.1	8.1	8.0	7.6	5.5	4.5
logK_{ass}, F^-	24.8	24.0	20.9	15.9	11.7	4.7
logK_{ass}, $H_2PO_4^-$	10.3	10.3	10.3	10.1	8.9	4.9
logK_{ass}, HSO_4^-	5.2	5.2	5.2	5.2	4.7	low

The predicted log$K$ values in Table 4 indicate that low water content in the solvent does not cause notable changes in anion binding strength for receptor RM1 in acetone. High solvent water content, however, has a notable effect on the predicted binding affinities.

3.1.3 Conformer stability in solution environment

To test, whether COSMO-RS as a method can correctly predict the most stable conformer in solvent environments, in work [III], the conformer stability of 105 small molecules in different solvents was investigated with COSMO-RS. The computational results were compared with experimental results from 20 literature sources.[79–98]

Accurate computational estimation conformer weights, especially, correctly recognizing the most stable conformer(s), is very important as it is necessary for correctly predicting free energies of species in the studied environment. The computational predictions of conformer stability strongly depend on the number of identified potential conformations submitted to the computational investigation. A computational method cannot predict the stability of a conformer that has not been recognized and submitted for calculation; but submitting too large number of conformers can also cause the misestimation of conformer weights. For large receptor molecules, especially if the molecular structure includes long and flexible groups, the conformer treatment is a complex and time-consuming task.[52]

Molecules for this study were chosen by these criteria:

- Well-defined conformational geometries exist for the molecule.
- Experimental data has been published that sufficiently describes the geometries of the most stable conformers of the molecule in the chosen solvent environment.
- The literature sources give enough information about the experimental conditions of the investigation of conformer stability (temperature, solvent

composition), so that it is possible to replicate these conditions in calculations.

Some examples follow.

In a set of 6 thiosemicarbazone molecules (Scheme 2), all have one intramolecular hydrogen bond in their preferred conformation, according to the experiments.[88,89] This was correctly predicted also by the computational study. The most stable conformers are shown on Scheme 2, the location of HB interactions is noted with purple lines.

In the case of two aldehyde molecules (RM11 and RM12, Scheme 3), COSMO-RS correctly (i.e. in accordance with experiments) predicted the preferred location of intramolecular HBs in the molecules, in which multiple possibilities for intramolecular HB formation exist.[87] The two possible HB locations are shown in Scheme 3. The most stable conformers are noted by green borders around the images and HB interactions are noted with purple lines.

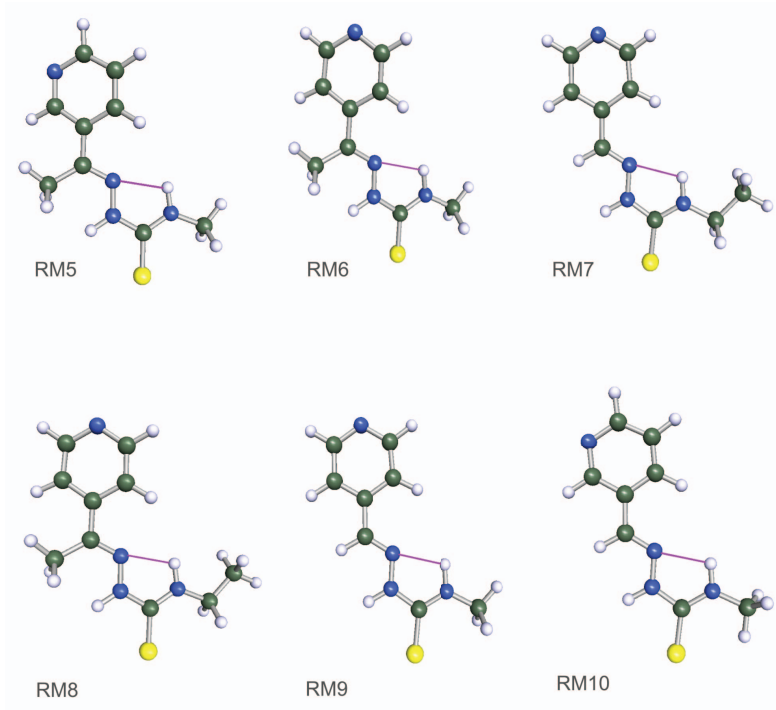

Scheme 2. Preferred conformations of thiosemicarbazone molecules RM5-RM10. Experimental data from ref. 88,89.

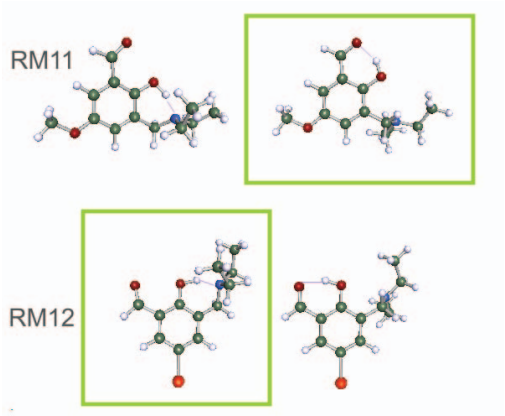

Scheme 3. Predicting the preferred HB formation inside a molecule (RM11 and RM12). Experimental data from ref. 87.

The results of work (III) showed that in the large majority of cases (103 out of 105), COSMO-RS predicted the dominant conformer, as well as existence and location of intramolecular hydrogen bond interactions inside molecules (when these occurred), correctly. On one occasion, the complete match between the computationally and experimentally determined stable conformer geometries could not be confirmed as the conformation of certain flexible side groups in the molecule was not described in the respective literature source. For another molecule, a problem arose with the geometry optimization at the DFT level of computations – the conformer described in the experimental study could not be reproduced computationally.

It is important to note that while the COSMO-RS method can generally predict the most stable conformer in the chosen environment accurately, the results of work [III] indicate that the method cannot accurately predict the exact numerical conformer weights. As the prediction of the ratio of conformers is very sensitive to the difference of Gibbs free energies between conformers, even a small change in the Gibbs free energies can cause large misestimations of conformer weights.

Overall, it can be concluded that for the study of small molecules, COSMO-RS method can in the majority of cases correctly predict the most stable conformer in a chosen solvent environment.

3.2 Computational receptor design

Works [II] and [IV] investigate the design and characterization of anion-selective receptors composed of the building blocks of the small receptors studied in work [I]. COSMO-RS calculations were used to determine the computational geometries of the most stable complexes in a chosen solvent environment (some examples are shown in Scheme 4) and to find out whether at least the order of binding affinities can be determined with this method.

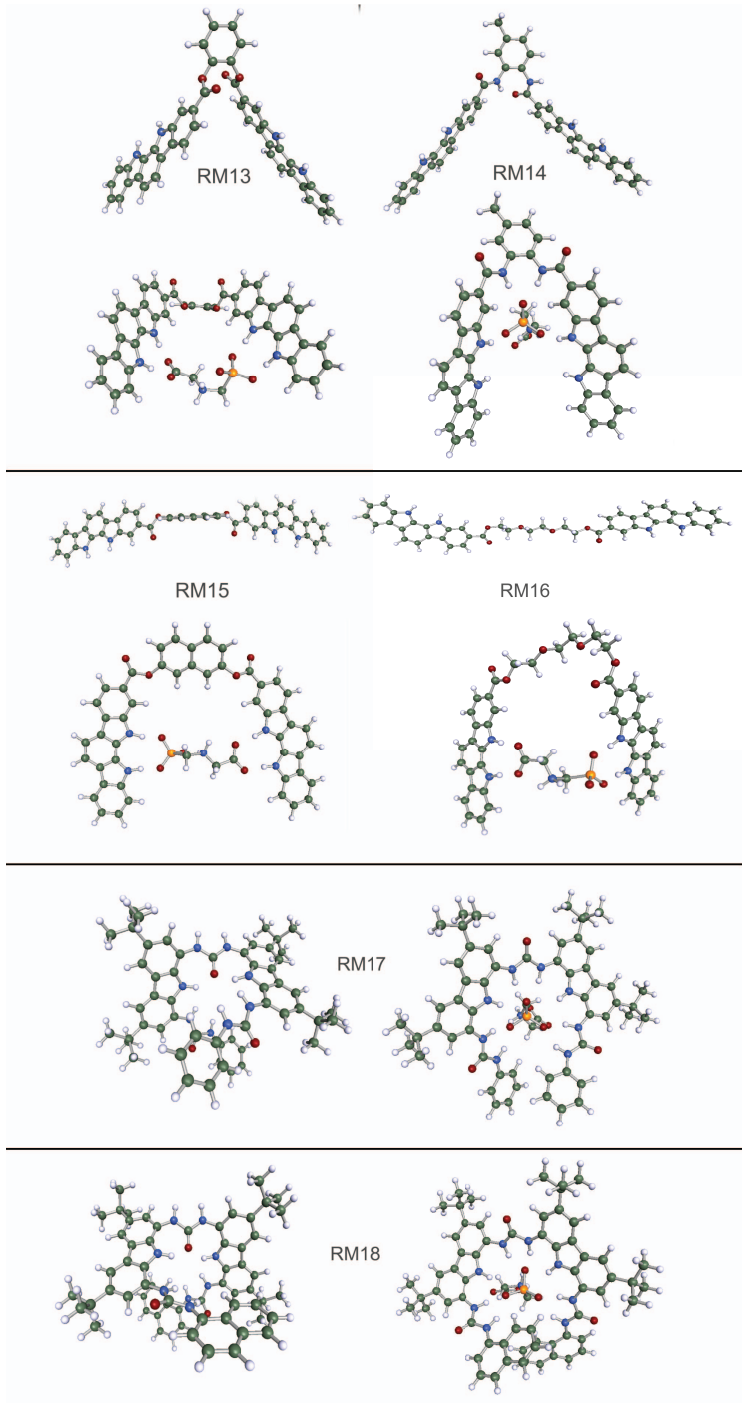

Scheme 4. Geometries of the most stable conformers of RM13, RM14, RM15, RM16, RM17, RM18 and the respective Gly^{2-} complexes in solution (receptors 2,4,6,8,16 and 17 in work [II] respectively).

3.2.1 Indolocarbazole-, carbazole- and urea-based receptors and effects of linker fragments

The purpose of the work [II] was to investigate the possibility of connecting several small anion receptor moieties together via a suitable linker fragment and to investigate how the use of various linker fragments of different lengths and rigidities would affect the strength of binding dianions. Altogether 12 larger receptors mostly based on the indolocarbazole moiety (and some on urea and carbazole fragments) used as binding groups and different connecting linker fragments are studied.

The focus of the receptor design was to create a receptor that is able to bind the glyphosate dianion (Gly^{2-}, the most stable form of glyphosate at neutral pH, Scheme 5).

Glyphosate (N-phosphonomethylglycine) is widely used as an active ingredient in herbicides around the world (commonly known under the commercial name Roundup).[99] The molecule is an amino acid that dissociates in three steps in aqueous solution and can take different forms depending on the pH of the solvent environment (see Scheme 5).[100]

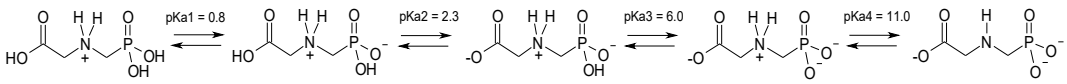

Scheme 5: Glyphosate in solution at different pH values.[100]

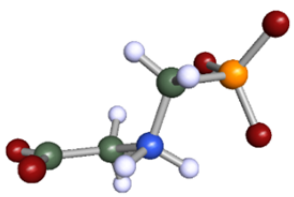

Scheme 6. Preferred geometry of Gly^{2-} anion in solution.

In a neutral environment, the majority of glyphosate will be predominantly in the dianionic form, Gly^{2-}. In order to selectively bind Gly^{2-}, the following characteristics of this dianion are important for designing a suitable receptor molecule candidate:

- The anionic centers of glyphosate are similar to acetate and alkylphosphonate anions (RPO_3^{2-}). Ideally, both anionic centers of glyphosate should be able to form multiple hydrogen bonds with the receptor. The binding groups of the receptor should have suitable geometry to allow strong hydrogen bond interactions to occur.

- The glyphosate dianion is not planar in its preferred conformation. Investigation of the preferred conformation of the glyphosate dianion in solution (Scheme 6) indicates that the plane of the oxygen atoms of the phosphonate group and the O-C-O plane of the carboxylate group intersect under a 90° angle and none of the three O-P-O planes are aligned with the O-C-O plane. This indicates that glyphosate may be able to bind better to receptors where the binding groups of the receptor are also not aligned in the same plane with one another. This can cause problems for the indolocarbazole-based receptor candidates as the indolocarbazole-small linker fragment-indolocarbazole structure tends to yield molecules with quite planar preferred geometries (e.g. Scheme 4, RM15).
- To avoid large energy penalties, the free receptor molecule should have a preferred conformation similar to the geometry of the receptor-Gly^{2-} complex (suitable receptor preorganization).

For the majority of the designed receptor candidates in work [II], indolocarbazole fragments were used as binding groups. The main reason for this is the rigidity of the indolocarbazole fragment and the suitability of the spatial arrangement of the N-H donor sites for both carboxylate and phosphonate moieties. Choice of a rigid binding fragment allows to study the contribution of the length and flexibility of the linker group used to connect the binding fragments in the structure of the receptor. The purpose of using two binding fragments in the receptor structure was to attempt to bind the glyphosate dianion from both of its anionic centers (an example is shown on Scheme 4 with RM13, RM14, RM15 and RM16 glyphosate complexes) but at the same time to use relatively simple receptors. Two additional receptors based on urea and carbazole fragments, initially introduced in a 2013 paper by Sanchez et al[101] (RM17 and RM18, Scheme 4) were also studied in this work. These receptors differed from the binding group-linker-binding group structure used in the design of the other receptors, and instead had a larger number of binding groups and no clear linker fragments in the receptor. As these receptors have a more complex structure and the glyphosate anion has a large number of binding groups to potentially interact with, it was studied how the Gly^{2-} anion would bind to a receptor of this type.

However, the results of this study show that this type of receptor design and prediction of binding is more complex than initially estimated and the binding affinities are not well predictable from the structure of the receptor. The computational receptor-glyphosate binding constant values are presented in Table 5 with experimental values (not measured by the author) for comparison.

Table 5. Experimental and computational logK_{ass} values for five receptor-glyphosate complexes [II].

Solvent:	logK_{ass}	RM13	RM14	RM15	RM16	RM17	RM18
DMSO, 0.5% H_2O	Exp.	5.1	5.9	3.6	4.7	4.8	high[a]
	Calc.	**18.6**	**13.3**	**17.5**	**21.2**	**22.0**	**23.3**
DMSO, 10% H_2O	Exp.	4.0	4.1	2.7	3.3	3.0	5.5
	Calc.	**11.7**	**6.7**	**10.0**	**14.4**	**13.4**	**14.8**

[a]The value was too high for experimental determination.

When looking at the values presented in Table 5, it can again be clearly seen that the COSMO-RS method cannot be used for the quantification of binding strength – not only are the binding constants overestimated by a large margin, but for this group of receptors the method also has failed to determine the binding order of the receptors.

Spectacularly, when comparing the experimental and computational values and trends in binding, receptor RM14 – having the second highest experimental binding affinity towards glyphosate – is suggested to be the weakest binder by COMSO-RS. This indicates that the approach has serious difficulties in predicting the behavior of host-guest complexes in complex situations with ionic centers, multiple hydrogen bonding sites and steric strain occurring inside the receptor.

When the linker fragment is rigid and the distance between the two IC binding groups is small, the glyphosate dianion does not fit inside the preferred conformation of the free receptor. In such cases, it is possible that in the preferred conformation of the formed receptor-anion complex, the glyphosate dianion is only bound into the complex via the phosphonate center. However, this type of complexation (e.g. with RM14) did not cause a comparative decrease in binding affinity, presumably because the anionic charge is largely concentrated on the phosphonate moiety. In fact, experimental logK_{ass} values shown in Table 5 indicate that RM14 has the second highest (after RM18) experimental binding affinity (logK_{exp} = 5.9) out of RM13 to RM18. As the geometry of the receptor in the complex allows both indolocarbazole binding groups and the HBD groups of the amide-based linker to form multiple hydrogen bond interactions with the phosphonate end of the glyphosate dianion, this receptor proved to exhibit the strongest binding affinity toward glyphosate out of all studied indolocarbazole-based receptors: its experimental logK_{ass} value was 0.8–2.3 log$K$ units higher than the other indolocarbazole-based receptors. Meanwhile, receptor RM15, which has a suitable distance between the indolocarbazole binding groups to allow the glyphosate dianion to fit between the binding groups and be bound from both anionic centers, exhibited the lowest binding affinity out of the studied receptors. This can tentatively be attributed to steric strain occurring inside the glyphosate dianion as the structure of the

receptor molecule is relatively planar in comparison to the preferred structure of glyphosate in its dianionic form (Scheme 6).

When a long and flexible linker fragment is used in the receptor structure (e.g. RM16 in Scheme 4), the free receptor has a large number of conformational choices, which introduces a large entropy penalty upon complex formation due to the large number of possible conformations in the free receptor. This means that the use of very long linkers may not be optimal even when it would seemingly allow the binding groups of the receptor to orient more suitably for the anionic centers of glyphosate in the receptor-anion complex. The experimental data from Table 5 indicates that receptor RM16 does not have a high binding affinity toward glyphosate compared to receptors RM13-RM15.

Work (II) also investigated two larger urea-based receptor structures: RM17 and RM18 (Scheme 4) that were initially proposed in ref 101. They differ by their structures from the other receptors studied in work [II] as they lack clearly distinguishable linker groups and binding groups and have a large number of HBD groups in their structure. While these receptors bind glyphosate only by the phosphonate group, the configuration of hydrogen bonds (especially in the case of receptor RM18, where it is likely caused by the attraction of the naphthalene groups at the ends of the molecule closing the receptor into a cavity-like structure), is very suitable for the geometry of the phosphonate group, allowing a total of 8 hydrogen bond interactions to form between the receptor and anion. Among the studied 12 receptor candidates in work [II], receptor RM18 was found to bind glyphosate the strongest.

When designing a receptor that contains both HBD and HBA groups, the possibility of intramolecular hydrogen bond (IMHB) interactions in the free receptor is important. Depending on the receptor structure, this can help or hinder binding, depending on the receptor geometry caused by the intramolecular HB interaction. When IMHB formation causes the free receptor to have a different geometry than that of the receptor-anion complex, or when the intramolecular HB involves a NH group important for binding the anion, the effects on binding affinity are negative. If the formation of IMHBs causes receptor preorganization to a geometry similar to that of the bound receptor, it may even enhance the binding strength. IMHB is present in the unbound receptors RM14, RM17 and RM18. RM14 and RM18 are among the best binders for Gly^{2-}, thus, in this case, IMHB has not had a strong negative effect on the binding ability.

It is important to note that the binding strength of receptor-glyphosate complexes also strongly depends on the surrounding solvent environment. Experimental study of these receptors by our group in work [II] showed that at higher solvent water content, the binding affinity of these receptors for glyphosate decreases markedly. This is caused by solvent effects – the preferential solvation of the receptor and especially anion with by water molecules, which stabilizes the free anion as opposed to the bound anion. This decrease of binding affinity is at least at qualitative level reproduced by COSMO-RS calculations (Table 5).

These are the main conclusions that can be drawn from work [II]:

- The relationship between linker length, linker rigidity and binding strength is not clear and cannot be computationally predicted by COSMO-RS. However, the choice of the linker fragment in the receptor does have a large effect on the strength of binding.
- Amide-based linker fragments may enhance binding strength through co-operativity effects, via additional hydrogen bonds.
- When the anion of interest has multiple anionic centers, steric compatibility between the anionic centers and the binding groups of the receptor is very important. If the receptor structure is very rigid, the anion may only be bound by one of its anionic centers when this results in less steric strain in the formed complex and a sufficient number of HB interactions.
- The binding affinity can be enhanced by interactions other than hydrogen bonding. For example, in some cases (e.g. RM17), the (solvophobic) interaction between the two naphthalene groups in the molecule helps with receptor preorganization.
- The geometry of the free guest is very important as well. For the glyphosate dianion, the two anionic centers are arranged almost perpendicularly to each other, which makes the indolocarbazole-linker-indolocarbazole structure less ideal for binding due to steric strain.
- In order to efficiently bind Gly^{2-} by both anionic centers, more complex receptors are most probably needed than the ones used here.

3.2.2 Moving towards selective carboxylate receptor design

In a 2015 study by our group, a large number of indolocarbazole-, urea-, indole-, carbazole-, thiourea- and amide- based anion receptors were experimentally and computationally studied in DMSO (with 0.5% H_2O) to investigate the binding affinities toward lactate, benzoate, acetate and pivalate.[59] The study determined that the binding affinity largely depends on the basicity and size of the anion and the strength of anion-receptor binding generally followed the same order (lactate < benzoate < acetate < pivalate). This is caused by the hydrogen bonding interactions, which are largely responsible for the complex formation between these receptors and anions. As hydrogen bonds are strongly directional, it is important to account for the preferred geometries of the receptor and anion, and the complementarity of the geometries of the anion and the binding groups in the receptor.[59]

In 2017, another study of 22 acyclic urea-, carbazole- and indolocarbazole-based receptors investigated the binding affinity towards 11 monocarboxylate anions.[60] The conclusions of the study were largely similar to those of ref. 59.

For both the 2015 and the 2017 studies, all receptor-anion geometries were also studied computationally with the COSMO-RS method. Investigation of the complex geometries indicated that receptors based on carbazolylurea fragments can be constructed with a good spatial fit of the HB donor groups towards

carboxylate anions. These types of receptors and their carboxylate binding abilities have been studied in work [IV] and summarized in the following sections.

3.2.3 Macrocyclic receptors

Work [IV] focuses on developing and studying macrocyclic receptors for the creation and characterization of carboxylate sensing solid-contact ion-selective electrodes (ISEs) that could be used for the determination of carboxylate anions. The first step of this work is choosing suitable receptor design. Computations were used for the prediction of steric effects and in determining suitable fit between macrocyclic receptor cavities and the anions of interest – formate, acetate, lactate, benzoate and pivalate.

A total of 15 receptors based on the biscarbazolylurea moiety (and similar in structure of receptors RM17 and RM18 from work [II] and ref. 101) were investigated in work [IV], 12 of them macrocycles with the space near the binding site fully enclosed by an aliphatic linker chain of differing length (varying from 3 to 14 -CH_2- units, see Scheme 7). Although this arrangement does not exactly form a structural cavity in the true sense of this word, in the interest of brevity the term “cavity” is used below.

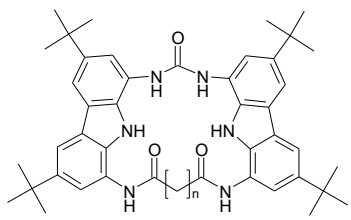

RM19 n = 3 **RM25** n = 9
RM20 n = 4 **RM26** n = 10
RM21 n = 5 **RM27** n = 11
RM22 n = 6 **RM28** n = 12
RM23 n = 7 **RM29** n = 13
RM24 n = 8 **RM30** n = 14

Scheme 7. Biscarbazolylurea-based receptors.

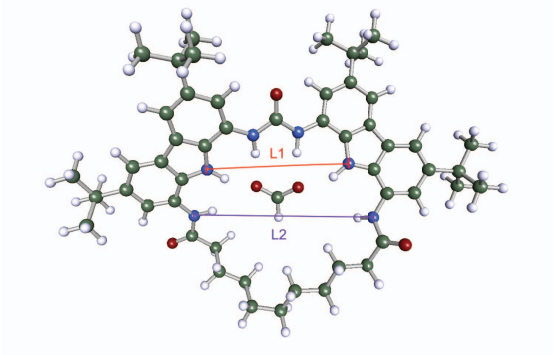

Scheme 8. Cavity size parameters L1 and L2.

Table 6. Receptor cavity size parameters L1 and L2 and the number of HB interactions in receptor-anion complexes according to COSMO-RS.

Receptor	L1 (Å) (carbazolyl NH distance)					L2 (Å) (amide NH distance)					Number of HB interactions in the complex				
Complex[a]	Ac	Bz	For	Piv	Lac	Ac	Bz	For	Piv	Lac	Ac	Bz	For	Piv	Lac[d]
RM19	**5.4**	**5.8**	**5.8**	**5.5**	**5.5**	**5.3**	**6.1**	**6.1**	**5.6**	**5.6**	**5**[b]	**5**[b]	**5**[b]	**5**[b]	**5**
RM20	5.4	5.4	5.5	5.4	5.7	5.6	5.6	5.7	5.6	5.9	5[b]	5[b]	5[b]	5[b]	5
RM21	**6.5**	**6.5**	**6.5**	**6.5**	**6.5**	**7.6**	**7.6**	**7.6**	**7.7**	**7.7**	**5**[b]	**5**[b]	**5**[b]	**5**[b]	**6**
RM22	6.7	6.7	6.7	6.6	6.7	8.3	8.4	8.3	8.0	8.2	5[b]	4[b]	4[b]	4[b]	4
RM23	**6.6**	**6.9**	**6.6**	**6.9**	**6.7**	**8.0**	**8.7**	**8.0**	**8.8**	**8.3**	**5**[b]	**4**[b]	**4**[b]	**4**[b]	**4**
RM24	6.8	7.1	7.3	6.8	7.2	8.5	9.4	9.7	8.4	9.2	4[b]	4[c]	4[c]	4[c]	6
RM25	**6.6**	**7.1**	**7.2**	**6.9**	**7.0**	**8.4**	**8.9**	**9.5**	**8.5**	**8.9**	**5**[b]	**4**[c]	**4**[c]	**4**[b]	**6**
RM26	6.8	7.1	7.3	7.0	7.1	8.7	9.1	10.1	8.9	9.0	4[b]	4[c]	4[c]	4[c]	4
RM27	**7.2**	**7.2**	**7.1**	**7.2**	**7.2**	**9.5**	**9.3**	**9.3**	**9.6**	**9.3**	**4**[c]	**4**[c]	**4**[c]	**4**[b]	**6**
RM28	6.8	6.8	6.8	7.2	7.4	8.7	8.4	8.5	9.8	10.2	4[b]	4[b]	4[b]	4[c]	4
RM29	**7.3**	**7.2**	**7.3**	**7.3**	**7.2**	**10.0**	**9.5**	**10.0**	**10.1**	**9.4**	**4**[b]	**4**[c]	**4**[b]	**4**[b]	**6**
RM30	6.8	7.4	6.8	7.0	6.9	8.8	10.3	8.8	8.9	8.9	4[b]	4[b]	4[b]	4[c]	6

The distance values for the receptors with an odd number of -CH_2- linker fragments are marked in bold. Receptors RM22 and RM24 displayed the highest binding affinities toward the studied anions.

[a] Ac – acetate; Bz – benzoate; For – formate; Piv – pivalate; Lac – lactate.

[b] The anion interacts with the linking groups sideways and interacts with one urea NH.

[c] The anionic COO^- group is oriented directly towards the urea fragment and interacts with both urea NH fragments in a matching spatial arrangement (each of the COO^- oxygens interact with the respective urea NH).

[d] Lactate binds into complex in a way that keeps the IMHB inside the anion (exception: RM30) and have a maximum number of HB interactions with the receptor.

Scheme 7 shows the structure of 12 macrocyclic receptors of varying cavity size that were studied in work [IV]. Table 6 presents information about the estimated receptor cavity sizes (see Scheme 8 for the definition of cavity size measurement parameters L1 and L2) and the computationally estimated number of HB interactions between the receptor-anion complexes. For estimating the number of HB interactions in the receptor-anion complexes, these criteria were used: max distance between HBD and HBA group: 2Å; minimal angle of HB formation: 90°.

Initially (receptors RM19 and RM20), the L1 and L2 parameters are rather similar to one another for all bound anions – when the macrocyclic cavity is very small, no anion can fit inside. For receptors RM21-RM30, the distance between amide NH groups (L2) mostly gradually increases (from 7.6 to 10.3 Å), but the distance between biscarbazolyl groups (L1) remains similar (6.7 to 7.4 Å). This is because of the relative structural rigidity of the biscarbazolyl groups in the receptor. Overall, receptors RM23 and RM25 (linker chain length of 7 and 9 $-CH_2-$ groups respectively) displayed the highest binding affinities toward all the studied anions. This indicates that size-based discrimination between these anions is not possible with macrocycles of this structure. The cause of the lack of size discrimination is likely the fact that even the larger anions can interact with the binding groups of the receptor without having to fit into the macrocyclic cavity (see Scheme 9 below).

An interesting trend is visible in the binding of formate anion and the L2 parameter. While the formate anion is the smallest in size out of all studied species, the L2 parameter for receptors RM22-RM30 (receptor amide NH group distance) is among the largest for the formate-receptor complexes. This indicates that only the formate anion can completely fit into the receptor cavity without deforming the receptor geometry. As an example, RM24 complexes with the studied anions are shown on Scheme 9.

For an additional comparison of complex geometries, the images of receptor-acetate complex geometries for RM19-RM30 are presented in Appendix 1.

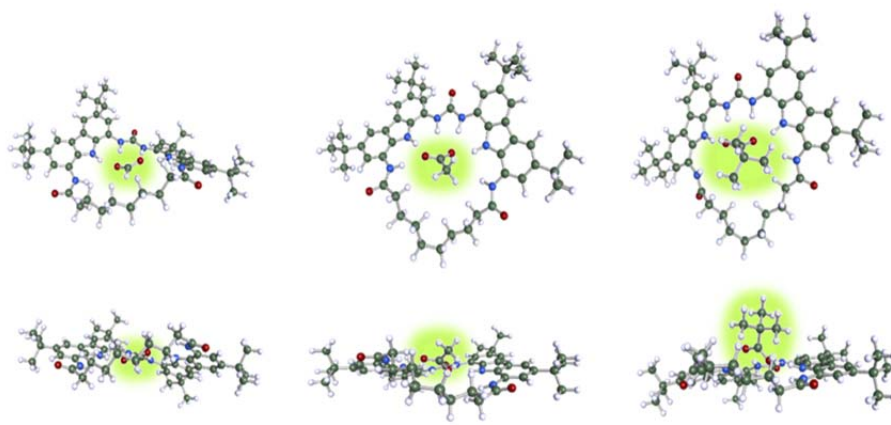

Scheme 9. RM24 complexes with formate, acetate and pivalate anions.

While the L1 and L2 parameters can be used to assess how much the macrocycle conformation differs in the complexes with various anions; they cannot be used to directly assess the fit of the anion inside the receptor. Even for the largest studied macrocyclic receptors (RM29 and RM30), benzoate and pivalate anions do not fit inside the receptor cavity, yet the cavity size parameters are quite similar to those of the other anion complexes. For the acetate and lactate complexes, while the anion fits close enough to the binding groups to interact with them and has a planar orientation with the binding groups of the receptor, complex formation will deform the preferred geometry of the linker chain in the macrocycle to make space for the anion. In comparison, formate, pivalate and benzoate cause less to no deformation in the linker chain geometry: formate fits into the receptor cavity, while benzoate and pivalate do not fit and thus bind with a different geometry. An example of formate, acetate and pivalate complexes of RM24 is shown on Scheme 9.

It is important to note that the preferred conformation of free receptor molecules depends on the cavity size. Scheme 10 displays the trend between linker length and the preference of IMHB interactions inside the receptor (in solvent DMSO with 0.5% H_2O) and Scheme 11 gives some examples of the optimal receptor geometries. For the smallest receptors (RM19-RM21), at least two IMHB interactions occur in the receptor and the urea fragment rotates its orientation to the outside of the receptor cavity. For RM22-24, the preferred free receptor geometry includes two IMHB interactions between the amide NHC=O oxygen atom and the NH hydrogen of the carbazole moiety. For the large receptors (RM25-RM30), the preferred geometry depends on the odd or even number of -CH_2- groups in the linker chain. The receptors with an even number of -CH_2- fragments in the linker have IMHB interactions between the amide NHC=O oxygen atom and the NH hydrogen of the carbazole moiety (generally one IMHB, except for RM26, which exhibits a 50–50 conformer balance of 1 and 2 IMHB interactions in the studied solvent environment). The receptors with an odd number of -CH_2- fragments prefer a geometry with no IMHB interactions. This conclusion is supported by the experimental binding affinity values – RM25 has an odd number of -CH_2- fragments in the linker and exhibits the highest binding affinity (both experimentally and computationally) toward the majority of the studied anions.

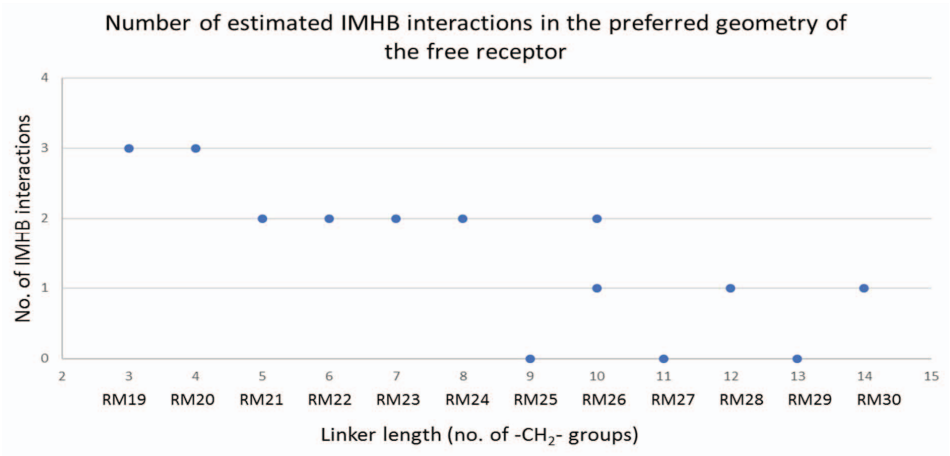

Scheme 10. Preference for IMHB interactions in the free receptor geometry in DMSO, 0.5% H_2O.

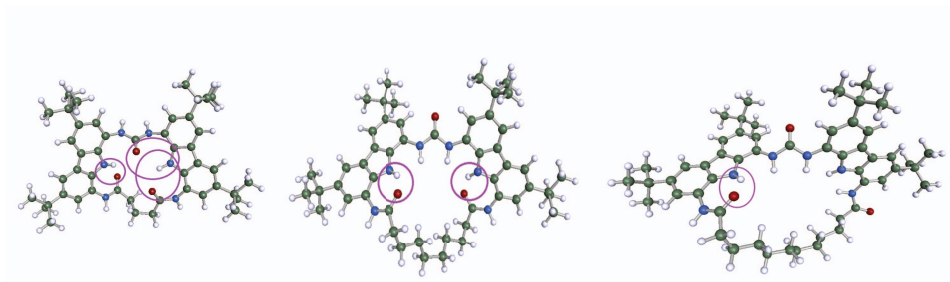

Scheme 11. IMHB interaction in the unbound macrocyclic receptors (RM19, RM24, RM26).

Generally, the experimental information obtained about receptor-anion complex geometry through ^{1}H NMR measurements conducted by our group (not the author) supports the most stable conformer predictions by COSMO-RS [IV]. Problems may occur in the study of receptor-anion complexation with very high steric strain in the receptor, which may be overestimated by COSMO-RS. For formate anion binding with receptors RM22 and RM23, experimental data indicated that in the receptor-formate complex, the anion should not interact with the receptor's amide NH groups, while the computationally determined most stable conformers indicated that the interaction exists in the complex.

The number of HB interactions in the optimal complex geometry (presented in Table 6) depends on the size of the anion and the size of the macrocycle. It can be seen that the smallest receptors generally have additional HB interactions with the anions (as the binding groups are located very close to one another, more of them can be reached by the anions simultaneously), but as the anions

are unable to orient themselves in a suitable way for strong hydrogen bond interactions with all available binding groups, the formed hydrogen bonds are weak and do not cause a comparative increase in the binding strength. The same can be said about lactate-receptor complexation – numerous suboptimal HB interactions do not result in strong binding. Benzoate and pivalate anions have an interesting trend in their preferences for HB interactions on complex formation – for the larger receptor molecules (RM27-RM30 for benzoate, RM24-RM30 for pivalate), the preferred complex geometry (which binding groups the large anions prefer to interact with to form the complex) depends on the length of the linker chain. This indicates once again that linker choice and preferred conformation has a strong influence on complex formation. For formate anion, it is evident that the anion binds to different binding groups depending on macrocyclic cavity size – for middle sized receptors (RM24 to RM27), formate interacts better with the urea NH groups, otherwise, the receptor-formate complex geometry is similar to the preferred geometry of acetate complexes.

Table 7. Experimental logK_{ass} values from work [IV] (not measured by the author of this thesis) and the comparison to computational predictions of COSMO-RS (parametrization BP_TZVP_20). Values in table are presented as logK_{ass},exp;logK_{ass},calc.

DMSO, 0.5% H_2O	Linker length	Acetate	Benzoate	Formate	Pivalate	Lactate
RM19	3	3.50;17.3 [a]	2.93;16.1 [a]	2.68;17.7 [a]	3.69;16.1 [a]	2.40;13.1 [a]
RM20	4	4.47;14.5 [a]	3.69;13.0 [a]	3.48;14.1 [a]	4.9;13.6 [a]	2.99;8.7 [a]
RM21	5	5.00;15.2 [a]	4.17;13.8 [a]	4.06;15.3 [b]	4.93;13.9 [a]	3.36;14.5 [a]
RM22	6	5.17;17.3 [a]	4.47;13.6 [a]	4.51;16.7 [c]	4.9;13.5 [a]	3.47;11.3 [a]
RM23 [d]	7	**5.69;**18.6 [a]	4.91;12.8 [a]	**4.80**;**18.3** [c]	5.64**;**12.2 [a]	4.04;11.7 [a]
RM24 [d]	8	5.34;15.7 [b]	4.64;15.0 [a]	4.63;16.4 [c]	5.23;14.4 [a]	3.62;13.2 [b]
RM25 [d]	9	**5.69;20.7** [b]	**4.95;16.5** [a]	4.59;16.6 [c]	**5.82;**11.6 [a]	**4.07;15.9** [b]
RM26 [d]	10	5.36;20.2 [b]	4.58;15.5 [a]	4.18;16.6 [c]	5.21;**17.2** [a]	3.69;15.6 [b]
RM27	11	5.18;17.1 [b]	4.62;11.0 [a]	4.00;16.5 [c]	5.43;14.7 [a]	3.78;14.9 [b]
RM28	12	5.00;16.6 [b]	4.41;11.9 [a]	3.86;16.0 [c]	5.40;11.0 [a]	3.62;11.0 [b]
RM29	13	4.97;17.2 [b]	4.33;13.5 [a]	3.76;16.7 [c]	5.44;14.6 [a]	3.58;14.7 [b]
RM30	14	4.97;17.7 [b]	4.32;14.6 [a]	3.77;17.0 [c]	5.48;14.2 [a]	2.40;12.4 [b]

[a] Computational complex geometries indicate that the anion does not fit into the receptor cavity for this complex.
[b] Computational complex geometries indicate that the anion partially fits into the cavity, but the geometry of the linker chain has been modified by complex formation.
[c] Computational complex geometries indicate that the anion fully fits into the cavity.
[d] According to experiments and calculations, these receptors generally exhibited the highest binding affinities toward the studied anions; The highest logK_{ass} values have been marked in bold in the table.

When looking at the comparison of experimental and computational values (Table 7), it can be seen that while computational predictions may generally estimate the highest binding affinity to be near RM23 or RM25, similar to experiments, otherwise, the agreement between computational and experimental binding affinities is poor. The misestimation of binding affinity by computations is especially visible for the smallest (RM19) and largest (RM29-RM30) macrocyclic receptors, where they are predicted to bind anions better than a number of other studied receptors, which is not in agreement with experimental results. For RM19, it is possible that the computational approach overestimates the extent of HB interactions for this receptor (that more possible HB interactions equals stronger binding, even when their orientation is very suboptimal). For receptors RM29 and RM30, problems may be caused by the computational characterization of the steric strain related to the linker chain conformation.

While studying binding in DMSO-H_2O can provide interesting results for the characterization of receptor molecules, the binding in this solvent system is unable to model the behavior of the receptors in the real sensors (not prepared by the author). As is evident from work [IV], the sensitivity of the sensors using receptors RM21, RM25 and RM28 towards benzoate is higher than the sensitivity towards acetate, while the solution binding studies indicate the opposite. The difference is caused by the fact that when measuring with sensor, the environments inside the sensor membrane (low polarity polymer matrix), as well as around the free anion (water) are very different compared to the DMSO solution environment used for the binding studies.

The following conclusions can be made by comparing the computational receptor geometry characteristics (Table 6) and the experimentally determined binding affinity values towards the studied anions (Table 7):

- Small cavity size of the macrocycle leads to lower binding affinity. The anion is able to have strong HB interactions with fewer available binding groups when it cannot even partially fit inside the cavity of the receptor molecule. For receptors RM19 to RM23, the binding affinities increase with the size of the macrocycle.
- From a certain point, (linker lengths above 9 -CH_2- fragments), increasing cavity size does not increase the binding strength (the anion complexes of receptors RM27 to RM30 have relatively similar binding strength in comparison with one another). Eventually, further increase in the cavity size will not help the anion fit closer to the binding groups inside the receptor cavity but may introduce steric strain into the molecule from the conformation of the flexible -CH_2- linker chain closing the cavity.
- For all studied anions, the strongest binding affinities (studied in DMSO with 0.5% water) were observed towards receptors RM23 and RM25. This trend was observed for both the experimental data measured in our group and published in work [IV] and can also be seen (apart from the predictions for pivalate binding) in the trends of computational predictions of $\log K_{ass}$ values (Table 7). This was also true for the larger anions (pivalate,

benzoate), which do not entirely fit inside the macrocyclic cavity for complex formation. The fact that the macrocycles with the largest cavity size do not have higher binding affinities for larger anions can be attributed to the large flexibility of the linker chain. As the linker structure of receptors RM19 to RM30 is highly flexible, this allows anions of all sizes to bind relatively easily by bending the linker group. This indicates that the cavity size is not the determining parameter that should be studied for the determination of binding strength and that selective binding of anions is not possible with macrocyclic receptors of this structure.

II Experimental determination of thermodynamic parameters of complex formation

3.3 Choosing the model reaction

The aim of this part of the study (work [V]) was to investigate the applicability of low volume microcalorimetry for the experimental determination of enthalpy and entropy effects of a simple 1:1 binding reaction. The model reaction for the study should meet certain criteria. The reaction must be fast and have 1:1 stoichiometry, without side-processes (e.g. pronation-deprotonation), the reactant molecules or ions should be commercially available with a suitable level of purity, a large number of reliable experimental results for the enthalpy and entropy effects of the model reaction should exist in previously published literature sources.

While this work primarily focuses on the study of anion receptors, this part of the study has been carried out studying receptor-cation binding as no anion binding reaction was found that would meet the above criteria. As anion-receptor chemistry is a newer field than the study of cation complexation, no anion receptors have been studied as extensively by a large number of research groups. When only very limited previously determined experimental data exists for comparison, stoichiometry of the binding reaction may not be reliably known and it may be more difficult to ascertain whether differences between the experimentally determined results of this study and the past literature results arise from differences in experimental conditions or methods used or if they indicate problems with the experimental approach used in this study. Many anion receptors are not commercially available and obtaining the compounds of suitable purity for ITC experiments may be difficult.

Binding reactions between 18-crown-6-ether (18C6) and alkali and alkaline earth metal cations meet all the mentioned criteria. K^+ was chosen as the guest ion, because the reaction between K^+ and 18C6 has been extensively studied by numerous groups and has a rather low binding affinity, which is also common for the types of anion-receptor complexes studied in this work.[102] 18C6 and cation binding has been used as a model reaction for a number of past studies and the reaction stoichiometry is well known to be 1:1.

The binding reaction of 18C6 and K^+ has been widely investigated in past studies from 1970s to 2000s (Table 8). The literature values of 1.97...2.14 ($\log K_{ass}$) and -23.4...-32 (ΔH) are presented in past studies.[50,103–109] While the experimentally determined association constant values are relatively similar between all sources, there are large differences in the estimates of reaction enthalpy, and these values are often accompanied by very low uncertainty estimates, which cannot account for a discrepancy of this magnitude.

Table 8. Literature data for ΔH and K_{ass} estimates for 18-crown-6-ether and K^+ binding.[50,103–109][V]

Ref.	Year	logK_{ass}	U (logK_{ass})	ΔH (kJ/mol)[ab]	U (ΔH)	Uncertainty type
[103]	1976	2.03	0.1	-25.8	0.04	s
[104]	1982	2.14	0.02	-23.4	0.84	$s \times t_{coeff}$
[105]	1987	1.97	0.05	-26.0	0.29	±x
[106]	1992	2.04	0.1	-26.3	0.2	$3 \times s$
[107]	1993	2.037	0.004	-24	0.4	±x
[108]	1995	2.06	0.02	-26	0.1	±x
[50]	2003	2.01 ... 2.1	0.01 ... 0.03	28.4 .... -32	0.3 ... 1.2	$2 \times s$
[109]	2008	2.1	0.08	-25	1.3	±x

[a] All ΔH values were determined with various calorimetric methods. For Ref. 104, K_{ass} was determined using potentiometry.
[b] When the literature estimates in original sources were presented in kcal/mol, the units were converted to kJ/mol by multiplying with 4.184.

3.4 Planning ITC experiments

The following points should be considered when choosing the experimental conditions for ITC studies of systems of low binding affinity.

- Choosing the "*c*" value. For low binding affinity systems, it is probable that the experiment will be conducted under low "*c*" value conditions. For low "*c*" experiments, additional attention should be paid to the following experimental parameters: sufficient extent of complexation at the end of experiment, careful consideration of chosen experimental concentrations, prior knowledge of reaction stoichiometry may be necessary.
- Extent of host-guest complexation by the end of the experiment. Ideally, more than 50% of the host molecules should be bound with the guest. When only a small part of the host in the calorimeter cell can be bound into the complex, only a part of the titration curve can be used for the prediction of reaction parameters and this will increase errors in the estimation of K_{ass}.
- Reaction stoichiometry. This is especially important for low "*c*" conditions, as under these conditions *n* and ΔH values have been found to strongly correlate[50] and curve fitting to determine the values of *n* and ΔH simultaneously is thus unadvisable. When the stoichiometry is known (especially when the known binding stoichiometry is 1:1 and the simple binding model can be used), the *n* value should be fixed for data treatment.
- Choice of host concentration in the cell and guest concentration in the syringe. A typical calorimetric experiment is often conducted by filling the calorimetric cell with low concentration (e.g. 1...10 mM) host compound solution and titrating it with the guest compound solution of 10–20 times higher concentration. This may not be ideal for low-affinity systems (low extent of receptor complexation at the end of experiment, low "*c*" parameter for the experiment). On the other hand, the choice of the guest concentration often has upper limits

(solubility, reasonable magnitude of the heat of dilution effect, larger risk of cross-contamination between experiments with the use of solutions with very high concentrations etc.). There are also limitations to using very low concentrations, as the accuracy of the measurements of very low heat effects is lower and effects of certain sources of measurement uncertainty (baseline stability, peak area integration accuracy, heat of dilution effects etc.) may influence the results proportionally more when low heat effects are studied.

- Magnitude of experimentally determined heat effects. The microcalorimeters work by applying and measuring small amounts of power to keep the temperature of the cell stable. When heat effects are too large for the instrument and drop below the level of reference power (negative values in the raw measurement data), it is outside the instrument's working area and the determined heat effects will be inaccurate and should thus not be used for data analysis. When heat effects are very small, the contributions of certain measurement uncertainty sources (peak integration and baseline stability, instrumental accuracy, accounting for the heat of dilution) increase notably.
- Purity of compounds. Calorimetric measurements can be quite sensitive to impurities in compounds and using compounds of insufficient purity (e.g. using a host or guest compound of 90% purity), will result in inaccurate determination of the thermodynamic parameters of the reaction.
- Heat of dilution effects. It is important to carry out two additional experiments every time to account for the heat of dilution effects for the syringe compound (titration experiment of syringe compound titrated to MQ water in cell) and for the cell compound (titration experiment of MQ water titrated to the compound in cell). With the use of low compound concentration in the cell, it is possible that heat effect of dilution is close to zero and can be ignored, but this should be experimentally checked. With low heat of dilution effects, care should be taken to study the obtained values to ensure that baseline deflections and systematic instrumental drift are not accounted for instead of the actual heat of dilution effects occurring in the solution.
- Good working order of the instrument. The proper working order of the calorimeter should be assessed regularly. This can be done by a number of various experiments. Certain model reactions can be studied and the obtained n, K_{ass} and ΔH values compared with reference values. Commonly, the reaction of Ca^{2+} and EDTA binding in MES buffer at a fixed pH value is used.[110] The instrument allows to carry out instrumental test of heat effect measurement by generating and measuring electrical pulses, the peak areas of which should fit inside ±1% of a given specification. MQ to MQ titration experiments carried out regularly will show cross-contamination or the need for additional cleaning for the calorimetric cell and syringe. For avoiding cross-contamination, it is also important to properly clean the syringe used for filling the calorimetric cell and to also regularly clean the overflow area above the cell compartment. The MQ water in the reference cell of the calorimeter should be changed often to ensure no contamination has occurred over time.

3.5 Basic principles of uncertainty estimation

Uncertainty estimation in work [V] was carried out using the component-by-component approach[111] in the following steps:

- Creating the mathematical model.
- Estimating the uncertainty contributions of input parameters.
- Calculating the standard uncertainties for experimentally determined heat effects (peak areas).
- Using the experimentally determined peak areas together with their uncertainty estimates and initial solution concentrations as input parameters for the python script, which is used to estimate the K_{ass} and ΔH values of the binding reaction.
- Component-by-component approach is used on equation (11), derived from equations (6) and (7)-(9), to determine the combined standard uncertainty for the experimental estimate of reaction enthalpy ΔH.

$$\Delta H = \frac{2Q}{nM_t V_0\left[1+\frac{X_t}{nM_t}+\frac{1}{nK_{ass}M_t}-\sqrt{\left(1+\frac{X_t}{nM_t}+\frac{1}{nK_{ass}M_t}\right)^2-\frac{4X_t}{nM_t}}\right]} \quad (11)$$

3.6 Estimating the uncertainty for input parameters

The standard uncertainties of input parameters were estimated:

- The standard uncertainty of solution concentrations (M_{t0}; c_{syr}) (making stock solutions, dilution, transfer) was conservatively estimated at 2% due to the very low concentrations involved.
- The standard uncertainty of volume delivery (V_{tot}, v_i) was estimated at 2%.
- The standard uncertainty of active volume (V_0) was estimated at 4 µl. The active volume of the iTC_{200} microcalorimeter is 200.6 µl.

3.7 The measurement uncertainty of the heat effects of single injections

In order to carry out data fitting, first, uncertainty estimation was carried out for the experimentally determined heat effects of the individual injections ΔQ(i) of the ITC experiment. An example for the determined uncertainty budgets for each injection for experiment K2 is displayed in Table 9.

It can be seen from Table 9 that the main contributors to the uncertainty of a single injection are the total injected titrant volumes V_{tot}(i) and V_{tot}(i-1).

Table 9. Uncertainty budgets for injections 1–20 for experiment K2.[a] [V, SI]

Inj. No	V_0	c_K	c_{18C6}	V_{tot} (i)	V_{tot} (i-1)
1	0%	**39%**	**21%**	**39%**	-
2	0%	**38%**	**23%**	**38%**	0%
3	0%	**20%**	14%	**42%**	**24%**
4	0%	**13%**	10%	**44%**	**33%**
5	1%	**9%**	8%	**45%**	**38%**
6	1%	6%	**7%**	**45%**	**41%**
7	1%	5%	**6%**	**45%**	**43%**
8	1%	4%	**5%**	**45%**	**44%**
9	2%	3%	**5%**	**45%**	**45%**
10	2%	2%	**5%**	**45%**	**46%**
11	2%	2%	**4%**	**45%**	**46%**
12	2%	1%	**4%**	**45%**	**47%**
13	3%	1%	**4%**	**45%**	**47%**
14	3%	1%	**4%**	**45%**	**47%**
15	3%	1%	**3%**	**45%**	**47%**
16	**4%**	1%	3%	**45%**	**47%**
17	**4%**	0%	3%	**45%**	**48%**
18	**4%**	0%	3%	**44%**	**48%**
19	**5%**	0%	3%	**44%**	**48%**
20	**5%**	0%	3%	**43%**	**48%**

[a] V_0 – active volume of the calorimetric cell; c_K – syringe concentration of guest (K^+); c_{18C6} – cell concentration of 18C6; V_{tot} (i) – total cumulative injection volume after injection i; V_{tot} (i-1) – total cumulative injection volume after injection i-1.

The three main contributors to the uncertainty of a given experimental heat effect are marked in bold.

The uncertainty contributions of v_i (volume of injection i) and V_{tot} (i-2) (total injection volume at injection i-2) were close to 0% for all injections and have been omitted from the table.

3.8 Determining the estimate of Δ*H* and estimating the combined standard uncertainty for the result

A python script was used for fitting the computational and experimental titration curves to determine the estimate for reaction enthalpy Δ*H*. The script takes initial K_{ass} and Δ*H* estimates, cell and syringe concentrations, injection volumes, experimentally determined heat effects (peak area values) and their standard uncertainties as input parameters and gives the estimates for K_{ass} and Δ*H* values for the input data together with an uncertainty estimate characterizing the fit. Details of the involved mathematics are given in work [V].

Table 10 shows the results of using the Python script with the data of 4 experiments (K1-K4). From the results of the four experiments, the combined standard uncertainty for ΔH was estimated from the mathematical model based on equation (11) (derived from equation (6)) (see section 3.5). The uncertainty budget for ΔH is presented in Table 11. According to the uncertainty budget, the most important components are the measured total heat effect of the experiment (Q_{tot}) and the initial 18C6 concentration in the cell M_{t0}. It must be noted that for our study, the n value was fixed, which was found to be necessary for calorimetric measurements under low-c conditions. Even a small error in the value of n (e.g. 3%) would increase the uncertainty estimate of ΔH by several times.

Table 10. Results of experiments K1-K4. The "c" parameter values for the experiments is 0.575.

Experiment	K1	K2	K3	K4
K_{ass}	69.2 (1.1)	69.2 (1.1)	70.8 (0.6)	70.5 (0.6)
ΔH	-27.6 (0.8)	-27.1 (0.8)	-25.8 (0.4)	-25.9 (0.4)

The combined standard uncertainty values obtained from the Python script are given in brackets.

Table 11. Uncertainty budget for the uncertainty of ΔH. [V]

Input quantities	Example values	Standard uncertainty of input value	Uncertainty components of ΔH (kJ/mol)	Contribution to ΔH uncertainty
Total heat Q_{tot}	-7.54 mJ	0.2 mJ	-0.7	40%
Association constant K_{ass}	69.9	2	0.0	17%
Active volume V_0	200.6 µl	4 µl	0.4	2%
Stoichiometry coefficient n	1	0	0.3	0%
Syringe conc. c_{syr} [a]	0.05 M	0.001 M	0.4	19%
Initial cell conc. M_{t0} [b]	0.005 M	0.0001 M	0.5	12%
Total injection volume V_{tot}	38.2 µl	0.764 µl	0.2	5%

[a] The parameter is used for the calculations of Xt, according to equations (9) and (10).
[b] The parameter is used for the calculation of Mt, according to equation (8).

Applying the component-by-component approach to uncertainty estimation (realized through the Kragten approach), the final result from experiments K1-K4 can be presented together with the combined standard uncertainty:

$$\Delta H = -27.1;\ u_c(\Delta H) = 1.1 \text{ kJ/mol}.$$

This result overlaps with the results of individual experiments in the limits of measurement uncertainty.

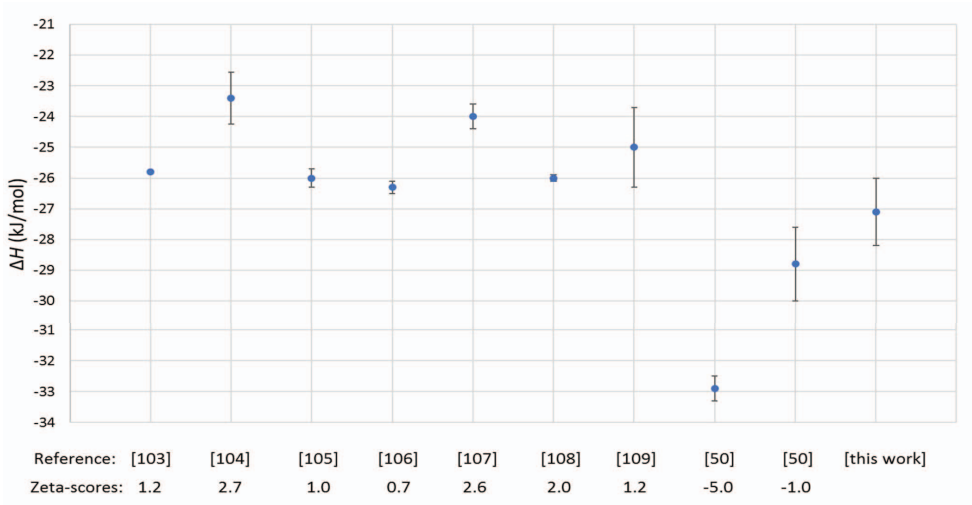

Scheme 12. Comparison of the results of this work with literature. Zeta scores with absolute values 2.0 or below indicate agreement between results.

The comparison of the result of our work with literature values is presented in Scheme 12. The zeta scores can be used for evaluating the agreement between the current results and values from the literature.[112] Zeta scores with absolute values 2 or below indicate agreement between results, absolute values between 2 and 3 indicate inconclusive situations, absolute values above 3 indicate disagreement. It can be seen that with our measurement uncertainty estimate, the result overlaps with the majority of the literature values in the limits of measurement uncertainty. Looking at the zeta-scores for the results, the values indicate that with two of the values (ref. 104, 107) the result is inconclusive and the lowest estimate of ref. 50 is in disagreement with our result. Importantly, the absolute values of these zeta scores might be rather over- than underestimated, as for the majority of literature values, instead of combined standard uncertainty estimates, just the standard deviations of replicate measurements were used. This indicates that the cause of discrepancy between literature values may not be in the inaccuracy of the measured results, but in the underestimation of measurement uncertainty.

SUMMARY

In the first part of the work, the possibility of investigating anion-receptor binding with the COSMO-RS computational method was studied in order to study and improve receptor design for a selection of analytically important anions (e.g. the glyphosate dianion and small monocarboxylate anions). The emphasis of the study focused on investigating the steric effects of binding and identifying the abilities and limitations of using the COSMO-RS approach for predicting receptor-anion binding affinities and for the computational characterization of anion receptors.

In order to test COSMO-RS for the ability to correctly estimate the most stable conformer in a chosen solvent environment, a test set of 105 small molecules was studied. In the majority of cases (103 out of 105), the method correctly predicted the most stable conformer of the studied molecule.

A number of small indolocarbazole- and urea- based molecules were studied to determine the ability of COSMO-RS to correctly determine the binding strength of anion-receptor complexes. It was found that COSMO-RS is unable to predict the absolute values of binding constants of anion-receptor complexes, while the overall trends in binding affinity of simple receptors are in most cases satisfactorily predicted by the method.

Next, the small indole, carbazole, indolocarbazole and urea fragments were used as building blocks to construct larger receptor molecules. These molecules were computationally studied – both linear molecules with the binding groups connected by various alkali or cyclic linking groups and molecules with macrocyclic structures were investigated.

These observations were made from the computational study of receptor design of varying linker length:

- The geometry of the anion and preferred free receptor conformation should be spatially suitable for one another. The positions of the binding groups as well as the linker length and rigidity affect binding affinity but do not always have a clearly predictable relationship.
- Steric effects are very important in determining the strength of binding. It is possible that high steric strain causes a dianion to prefer binding into a complex by only one of its anionic centers.
- The COSMO-RS method can in most cases be used to estimate the geometric parameters of receptors and receptor anion complexes – preferred conformations, whether something is “small enough” or “big enough”, whether HB donors and HB acceptors are sufficiently close, etc.
- The COSMO-RS method in general cannot be used for prediction of binding affinity ($\log K_{ass}$ values) for receptor-anion binding. The absolute values of binding constant $\log K_{ass}$ values for anion receptors are overestimated by large margins for even very simple systems. In the case of more complex systems, even trends in $\log K_{ass}$ values cannot be reliably predicted.

For macrocyclic receptors, the binding strength is affected by the size of the cavity and the anion, but it is not straightforward to predict for all anions. While the smallest anions can fit inside smaller cavities and large anions cannot, the results of the study indicate that effective discrimination of anions by size alone is not possible for macrocyclic receptors of this structure. As the structure uses a flexible linker fragment (an alkyl chain of varying length), the larger anions are able to form a complex when the alkyl chain bends out of the way and, as a result, for the group of studied macrocyclic receptors, two receptors with a middle-sized cavity exhibited the strongest binding affinities towards all studied anions.

The second, experimental part of the work investigates the possibility of studying the thermodynamic parameters, first of all, binding enthalpy, of low-affinity host-guest binding reactions using a small-volume microcalorimeter. A thorough uncertainty estimation is carried out to determine the main uncertainty sources and to estimate the measurement uncertainty of reaction enthalpy estimates determined using ITC. The study presents suggestions on experiment planning for the study of low-affinity systems and concludes that enthalpy determination is possible with a combined standard uncertainty in the range of 1–2 kJ/mol. The biggest contributors to the measurement uncertainty of reaction enthalpy ΔH were determined to be the determination of the total heat effect of the reaction and the reagent concentrations.

REFERENCES

(1) Gale, P. A.; Howe, E. N. W.; Wu, X. Anion Receptor Chemistry. *Chem* **2016**, *1* (3), 351–422. https://doi.org/10.1016/j.chempr.2016.08.004.

(2) Diehl, K. L.; Anslyn, E. V. Array Sensing Using Optical Methods for Detection of Chemical and Biological Hazards. *Chem. Soc. Rev.* **2013**, *42* (22), 8596. https://doi.org/10.1039/c3cs60136f.

(3) Teresa Albelda, M.; Frías, J. C.; García-España, E.; Schneider, H.-J. Supramolecular Complexation for Environmental Control. *Chem. Soc. Rev.* **2012**, *41* (10), 3859. https://doi.org/10.1039/c2cs35008d.

(4) Kolesnichenko, I. V.; Anslyn, E. V. Practical Applications of Supramolecular Chemistry. *Chem. Soc. Rev.* **2017**, *46* (9), 2385–2390. https://doi.org/10.1039/C7CS00078B.

(5) Culver, H. R.; Sharma, I.; Wechsler, M. E.; Anslyn, E. V.; Peppas, N. A. Charged Poly(N-Isopropylacrylamide) Nanogels for Use as Differential Protein Receptors in a Turbidimetric Sensor Array. *Analyst* **2017**, *142* (17), 3183–3193. https://doi.org/10.1039/C7AN00787F.

(6) Hein, R.; Beer, P. D.; Davis, J. J. Electrochemical Anion Sensing: Supramolecular Approaches. *Chem. Rev.* **2020**, *120* (3), 1888–1935. https://doi.org/10.1021/acs. chemrev.9b00624.

(7) Brooks, S. J.; García-Garrido, S. E.; Light, M. E.; Cole, P. A.; Gale, P. A. Conformational Control of Selectivity and Stability in Hybrid Amide/Urea Macrocycles. *Chem. Eur. J.* **2007**, *13* (12), 3320–3329. https://doi.org/10.1002/chem.200601647.

(8) Assaf, K. I.; Ural, M. S.; Pan, F.; Georgiev, T.; Simova, S.; Rissanen, K.; Gabel, D.; Nau, W. M. Water Structure Recovery in Chaotropic Anion Recognition: High-Affinity Binding of Dodecaborate Clusters to γ-Cyclodextrin. *Angew. Chem. Int. Ed.* **2015**, *54* (23), 6852–6856. https://doi.org/10.1002/anie.201412485.

(9) Pancholi, J.; Beer, P. D. Halogen Bonding Motifs for Anion Recognition. *Coordination Chemistry Reviews* **2020**, *416*, 213281. https://doi.org/10.1016/j.ccr.2020.213281.

(10) Schneider, H.-J. Strain Effects Determine the Performance of Artificial Allosteric Systems: Calixarenes as Models. *Chem. Commun.* **2019**, *55* (24), 3433–3444. https://doi.org/10.1039/C9CC00573K.

(11) Steed, J. W.; Turner, D. R.; Wallace, K. J. *Core Concepts in Supramolecular Chemistry and Nanochemistry*; John Wiley: Chichester, England ; Hoboken, NJ, 2007.

(12) Schneider, H.-J. Binding Mechanisms in Supramolecular Complexes. *Angewandte Chemie International Edition* **2009**, *48* (22), 3924–3977. https://doi.org/10.1002 /anie.200802947.

(13) Anslyn, E. V. Supramolecular Analytical Chemistry. *The Journal of Organic Chemistry* **2007**, *72* (3), 687–699. https://doi.org/10.1021/jo0617971.

(14) Fabbrizzi, L.; Francese, G.; Licchelli, M.; Perotti, A.; Taglietti, A. Fluorescent Sensor of Imidazole and Histidine. *Chem. Commun.* **1997**, No. 6, 581–582. https://doi.org/10.1039/a608531h.

(15) Evans, L. S.; Gale, P. A.; Light, M. E.; Quesada, R. Pyrrolylamidourea Based Anion Receptors. *New J. Chem.* **2006**, *30* (7), 1019. https://doi.org/10.1039/b603223k.

(16) Folmer-Andersen, J. F.; Lynch, V. M.; Anslyn, E. V. “Naked-Eye” Detection of Histidine by Regulation of CuII Coordination Modes. *Chem. Eur. J.* **2005**, *11* (18), 5319–5326. https://doi.org/10.1002/chem.200500016.
(17) Curiel, D.; Cowley, A.; Beer, P. D. Indolocarbazoles: A New Family of Anion Sensors. *Chemical Communications* **2005**, No. 2, 236. https://doi.org/10.1039/b412363h.
(18) Schneider, H.-J.; Yatsimirsky, A. K. Selectivity in Supramolecular Host–Guest Complexes. *Chem. Soc. Rev.* **2008**, *37* (2), 263–277. https://doi.org/10.1039/B612543N.
(19) Wright, A. T.; Anslyn, E. V. Differential Receptor Arrays and Assays for Solution-Based Molecular Recognition. *Chem. Soc. Rev.* **2006**, *35* (1), 14–28. https://doi.org/10.1039/B505518K.
(20) Gale, P. A.; Camiolo, S.; Tizzard, G. J.; Chapman, C. P.; Light, M. E.; Coles, S. J.; Hursthouse, M. B. 2-Amidopyrroles and 2,5-Diamidopyrroles as Simple Anion Binding Agents. *J. Org. Chem.* **2001**, *66* (23), 7849–7853. https://doi.org/10.1021/ jo016020g.
(21) Bates, G. W.; Triyanti; Light, M. E.; Albrecht, M.; Gale, P. A. 2,7-Functionalized Indoles as Receptors for Anions. *J. Org. Chem.* **2007**, *72* (23), 8921–8927. https://doi.org/10.1021/jo701702p.
(22) Gale, P. A. Synthetic Indole, Carbazole, Biindole and Indolocarbazole-Based Receptors: Applications in Anion Complexation and Sensing. *Chem. Commun.* **2008**, No. 38, 4525. https://doi.org/10.1039/b809508f.
(23) Caltagirone, C.; Gale, P. A.; Hiscock, J. R.; Brooks, S. J.; Hursthouse, M. B.; Light, M. E. 1,3-Diindolylureas: High Affinity Dihydrogen Phosphate Receptors. *Chemical Communications* **2008**, No. 26, 3007. https://doi.org/10.1039/b806238b.
(24) Hiscock, J. R.; Gale, P. A.; Caltagirone, C.; Hursthouse, M. B.; Light, M. E. Fluorescent Carbazolylurea- and Carbazolylthiourea-Based Anion Receptors and Sensors. *Supramolecular Chemistry* **2010**, *22* (11–12), 647–652. https://doi.org/10.1080/10610271003637087.
(25) Grabowski, S. J. What Is the Covalency of Hydrogen Bonding? *Chemical Reviews* **2011**, *111* (4), 2597–2625. https://doi.org/10.1021/cr800346f.
(26) Biedermann, F.; Uzunova, V. D.; Scherman, O. A.; Nau, W. M.; De Simone, A. Release of High-Energy Water as an Essential Driving Force for the High-Affinity Binding of Cucurbit[*n*]Urils. *J. Am. Chem. Soc.* **2012**, *134* (37), 15318–15323. https://doi.org/10.1021/ja303309e.
(27) Chen, L.; Berry, S. N.; Wu, X.; Howe, E. N. W.; Gale, P. A. Advances in Anion Receptor Chemistry. *Chem* **2020**, *6* (1), 61–141. https://doi.org/10.1016/j.chempr.2019.12.002.
(28) Langton, M. J.; Serpell, C. J.; Beer, P. D. Anion Recognition in Water: Recent Advances from a Supramolecular and Macromolecular Perspective. *Angew. Chem. Int. Ed.* **2016**, *55* (6), 1974–1987. https://doi.org/10.1002/anie.201506589.
(29) Sokkalingam, P.; Shraberg, J.; Rick, S. W.; Gibb, B. C. Binding Hydrated Anions with Hydrophobic Pockets. *J. Am. Chem. Soc.* **2016**, *138* (1), 48–51. https://doi.org/10.1021/jacs.5b10937.
(30) Yang, R.; Liu, W.-X.; Shen, H.; Huang, H.-H.; Jiang, Y.-B. Anion Binding in Aqueous Solutions by *N* -(Isonicotinamido)- *N* ‘-Phenylthiourea-Based Simple Synthetic Neutral Receptors. Role of the Hydrophobic Microenvironment of the Receptor Molecule. *J. Phys. Chem. B* **2008**, *112* (16), 5105–5110. https://doi.org/10.1021/jp711899h.

(31) Assaf, K. I.; Gabel, D.; Zimmermann, W.; Nau, W. M. High-Affinity Host–Guest Chemistry of Large-Ring Cyclodextrins. *Org. Biomol. Chem.* **2016**, *14* (32), 7702–7706. https://doi.org/10.1039/C6OB01161F.
(32) Lim, J. Y. C.; Marques, I.; Thompson, A. L.; Christensen, K. E.; Félix, V.; Beer, P. D. Chalcogen Bonding Macrocycles and [2]Rotaxanes for Anion Recognition. *J. Am. Chem. Soc.* **2017**, *139* (8), 3122–3133. https://doi.org/10.1021/jacs.6b12745.
(33) Gale, P. A. Anion and Ion-Pair Receptor Chemistry: Highlights from 2000 and 2001. *Coordination Chemistry Reviews* **2003**, *240* (1–2), 191–221. https://doi.org/10.1016/S0010-8545(02)00258-8.
(34) Lim, J. Y. C.; Beer, P. D. Sigma-Hole Interactions in Anion Recognition. *Chem* **2018**, *4* (4), 731–783. https://doi.org/10.1016/j.chempr.2018.02.022.
(35) Lande, D. N.; Gejji, S. P. Cooperative Hydrogen Bonding, Molecular Electrostatic Potentials, and Spectral Characteristics of Partial Thia-Substituted Calix[4]Arene Macrocycles. *The Journal of Physical Chemistry A* **2016**, *120* (37), 7385–7397. https://doi.org/10.1021/acs.jpca.6b07568.
(36) Schneider, H.-J. Limitations and Extensions of the Lock-and-Key Principle: Differences between Gas State, Solution and Solid State Structures. *International Journal of Molecular Sciences* **2015**, *16* (4), 6694–6717. https://doi.org/10.3390/ijms16046694.
(37) Evans, N. H.; Rahman, H.; Davis, J. J.; Beer, P. D. Surface-Attached Sensors for Cation and Anion Recognition. *Anal Bioanal Chem* **2012**, *402* (5), 1739–1748. https://doi.org/10.1007/s00216-011-5403-7.
(38) Schneider, H.-J. Quantification of Noncovalent Interactions – Promises and Problems. *New J. Chem.* **2019**, *43* (39), 15498–15512. https://doi.org/10.1039/C9NJ03325D.
(39) Tellinghuisen, J. Critique of Methods for Estimating Heats in Isothermal Titration Calorimetry. *Analytical Biochemistry* **2018**, *563*, 79–86. https://doi.org/10.1016/j.ab.2018.08.015.
(40) Tellinghuisen, J. Optimizing Experimental Parameters in Isothermal Titration Calorimetry: Variable Volume Procedures. *J. Phys. Chem. B* **2007**, *111* (39), 11531–11537. https://doi.org/10.1021/jp074515p.
(41) Horn, J. R.; Brandts, J. F.; Murphy, K. P. Van't Hoff and Calorimetric Enthalpies II: Effects of Linked Equilibria. *Biochemistry* **2002**, *41* (23), 7501–7507. https://doi.org/10.1021/bi025626b.
(42) Horn, J. R.; Russell, D.; Lewis, E. A.; Murphy, K. P. Van't Hoff and Calorimetric Enthalpies from Isothermal Titration Calorimetry: Are There Significant Discrepancies? *Biochemistry* **2001**, *40* (6), 1774–1778. https://doi.org/10.1021/bi002408e.
(43) Kantonen, S. A.; Henriksen, N. M.; Gilson, M. K. Accounting for Apparent Deviations between Calorimetric and van't Hoff Enthalpies. *Biochimica et Biophysica Acta (BBA) – General Subjects* **2018**, *1862* (3), 692–704. https://doi.org/10.1016/ j.bbagen.2017.11.020.
(44) Liu, Y.; Sturtevant, J. M. Significant Discrepancies between van't Hoff and Calorimetric Enthalpies. II. *Protein Sci.* **1995**, *4* (12), 2559–2561. https://doi.org/10.1002/pro.5560041212.
(45) Mizoue, L. S.; Tellinghuisen, J. Calorimetric vs. van't Hoff Binding Enthalpies from Isothermal Titration Calorimetry: Ba2+-Crown Ether Complexation. *Biophysical Chemistry* **2004**, *110* (1–2), 15–24. https://doi.org/10.1016/j.bpc.2003.12.011.

(46) Naghibi, H.; Tamura, A.; Sturtevant, J. M. Significant Discrepancies between van't Hoff and Calorimetric Enthalpies. *Proceedings of the National Academy of Sciences* **1995**, *92* (12), 5597–5599. https://doi.org/10.1073/pnas.92.12.5597.
(47) Wiseman, T.; Williston, S.; Brandts, J. F.; Lin, L.-N. Rapid Measurement of Binding Constants and Heats of Binding Using a New Titration Calorimeter. *Analytical Biochemistry* **1989**, *179* (1), 131–137. https://doi.org/10.1016/0003-2697(89)90213-3.
(48) Grossoehme, N. E.; Spuches, A. M.; Wilcox, D. E. Application of Isothermal Titration Calorimetry in Bioinorganic Chemistry. *J Biol Inorg Chem* **2010**, 9.
(49) C., J.; Murciano-Calles, J.; S., E.; Iglesias-Bexiga, M.; Luque, I.; Ruiz-Sanz, J. Isothermal Titration Calorimetry: Thermodynamic Analysis of the Binding Thermograms of Molecular Recognition Events by Using Equilibrium Models. In *Applications of Calorimetry in a Wide Context – Differential Scanning Calorimetry, Isothermal Titration Calorimetry and Microcalorimetry*; Elkordy, A. A., Ed.; InTech, 2013. https://doi.org/10.5772/53311.
(50) Turnbull, W. B.; Daranas, A. H. On the Value of *c* : Can Low Affinity Systems Be Studied by Isothermal Titration Calorimetry? *Journal of the American Chemical Society* **2003**, *125* (48), 14859–14866. https://doi.org/10.1021/ja036166s.
(51) Tellinghuisen, J. Isothermal Titration Calorimetry at Very Low c. *Analytical Biochemistry* **2008**, *373* (2), 395–397. https://doi.org/10.1016/j.ab.2007.08.039.
(52) Mobley, D. L.; Gilson, M. K. Predicting Binding Free Energies: Frontiers and Benchmarks. *Annu. Rev. Biophys.* **2017**, *46* (1), 531–558. https://doi.org/10.1146/annurev-biophys-070816-033654.
(53) Durrant, J. D.; McCammon, J. A. Molecular Dynamics Simulations and Drug Discovery. *BMC Biol* **2011**, *9* (1), 71. https://doi.org/10.1186/1741-7007-9-71.
(54) Marenich, A. V.; Cramer, C. J.; Truhlar, D. G. Universal Solvation Model Based on Solute Electron Density and on a Continuum Model of the Solvent Defined by the Bulk Dielectric Constant and Atomic Surface Tensions. *The Journal of Physical Chemistry B* **2009**, *113* (18), 6378–6396. https://doi.org/10.1021/jp810292n.
(55) Assaf, K. I.; Florea, M.; Antony, J.; Henriksen, N. M.; Yin, J.; Hansen, A.; Qu, Z.; Sure, R.; Klapstein, D.; Gilson, M. K.; Grimme, S.; Nau, W. M. HYDROPHOBE Challenge: A Joint Experimental and Computational Study on the Host–Guest Binding of Hydrocarbons to Cucurbiturils, Allowing Explicit Evaluation of Guest Hydration Free-Energy Contributions. *J. Phys. Chem. B* **2017**, *121* (49), 11144–11162. https://doi.org/10.1021/acs.jpcb.7b09175.
(56) Klamt, A.; Jonas, V. Treatment of the Outlying Charge in Continuum Solvation Models. *The Journal of Chemical Physics* **1996**, *105* (22), 9972–9981. https://doi.org/10.1063/1.472829.
(57) Klamt, A. *COSMO-RS: From Quantum Chemistry to Fluid Phase Thermodynamics and Drug Design*; Elsevier, 2005.
(58) Klamt, A.; Schüürmann, G. COSMO: A New Approach to Dielectric Screening in Solvents with Explicit Expressions for the Screening Energy and Its Gradient. *J. Chem. Soc., Perkin Trans. 2* **1993**, No. 5, 799–805. https://doi.org/10.1039/P29930000799.
(59) Kadam, S. A.; Martin, K.; Haav, K.; Toom, L.; Mayeux, C.; Pung, A.; Gale, P. A.; Hiscock, J. R.; Brooks, S. J.; Kirby, I. L.; Busschaert, N.; Leito, I. Towards the Discrimination of Carboxylates by Hydrogen-Bond Donor Anion Receptors. *Chem. Eur. J.* **2015**, *21* (13), 5145–5160. https://doi.org/10.1002/chem. 201405858.

(60) Martin, K.; Nõges, J.; Haav, K.; Kadam, S. A.; Pung, A.; Leito, I. Exploring Selectivity of 22 Acyclic Urea-, Carbazole- and Indolocarbazole-Based Receptors towards 11 Monocarboxylates: Exploring Selectivity of 22 Acyclic Urea-, Carbazole- and Indolocarbazole-Based Receptors towards 11 Monocarboxylates. *Eur. J. Org. Chem.* **2017**, *2017* (35), 5231–5237. https://doi.org/10.1002/ejoc.201700931.

(61) Klamt, A.; Eckert, F.; Arlt, W. COSMO-RS: An Alternative to Simulation for Calculating Thermodynamic Properties of Liquid Mixtures. *Annual Review of Chemical and Biomolecular Engineering* **2010**, *1* (1), 101–122. https://doi.org/10.1146/annurev-chembioeng-073009-100903.

(62) Skyner, R. E.; McDonagh, J. L.; Groom, C. R.; van Mourik, T.; Mitchell, J. B. O. A Review of Methods for the Calculation of Solution Free Energies and the Modelling of Systems in Solution. *Phys. Chem. Chem. Phys.* **2015**, *17* (9), 6174–6191. https://doi.org/10.1039/C5CP00288E.

(63) Carloni, P.; Rothlisberger, U.; Parrinello, M. The Role and Perspective of Ab Initio Molecular Dynamics in the Study of Biological Systems. *Acc. Chem. Res.* **2002**, *35* (6), 455–464. https://doi.org/10.1021/ar010018u.

(64) Tshepelevitsh, S.; Oss, M.; Pung, A.; Leito, I. Evaluating the COSMO-RS Method for Modeling Hydrogen Bonding in Solution. *ChemPhysChem* **2013**, *14* (9), 1909–1919. https://doi.org/10.1002/cphc.201300186.

(65) Klamt, A. The COSMO and COSMO-RS Solvation Models. *WIREs Comput Mol Sci* **2011**, *1* (5), 699–709. https://doi.org/10.1002/wcms.56.

(66) Balasubramani, S. G.; Chen, G. P.; Coriani, S.; Diedenhofen, M.; Frank, M. S.; Franzke, Y. J.; Furche, F.; Grotjahn, R.; Harding, M. E.; Hättig, C.; Hellweg, A.; Helmich-Paris, B.; Holzer, C.; Huniar, U.; Kaupp, M.; Marefat Khah, A.; Karbalaei Khani, S.; Müller, T.; Mack, F.; Nguyen, B. D.; Parker, S. M.; Perlt, E.; Rappoport, D.; Reiter, K.; Roy, S.; Rückert, M.; Schmitz, G.; Sierka, M.; Tapavicza, E.; Tew, D. P.; van Wüllen, C.; Voora, V. K.; Weigend, F.; Wodyński, A.; Yu, J. M. TURBOMOLE: Modular Program Suite for *Ab Initio* Quantum-Chemical and Condensed-Matter Simulations. *J. Chem. Phys.* **2020**, *152* (18), 184107. https://doi.org/10.1063/5.0004635.

(67) *TURBOMOLE, V6.2 2010; a Development of University of Karlsruhe and Forschungszentrum Karlsruhe GmbH, 1989–2007, TURBOMOLE GmbH, since 2007; Available from Http://Www.Turbomole.Com.*

(68) *TURBOMOLE, V6.4 2012; a Development of University of Karlsruhe and Forschungszentrum Karlsruhe GmbH, 1989–2007, TURBOMOLE GmbH, since 2007; Available from Http://Www.Turbomole.Com.*

(69) *TURBOMOLE, V6.5 2013; a Development of University of Karlsruhe and Forschungszentrum Karlsruhe GmbH, 1989–2007, TURBOMOLE GmbH, since 2007; Available from Http://Www.Turbomole.Com.*

(70) Perdew, J. P. Density-Functional Approximation for the Correlation Energy of the Inhomogeneous Electron Gas. *Phys. Rev. B* **1986**, *33* (12), 8822–8824. https://doi.org/10.1103/PhysRevB.33.8822.

(71) Becke, A. D. Density-Functional Exchange-Energy Approximation with Correct Asymptotic Behavior. *Phys. Rev. A* **1988**, *38* (6), 3098–3100. https://doi.org/10.1103/PhysRevA.38.3098.

(72) Franke, R.; Hannebauer, B. On the Influence of Basis Sets and Quantum Chemical Methods on the Prediction Accuracy of COSMO-RS. *Phys. Chem. Chem. Phys.* **2011**, *13* (48), 21344. https://doi.org/10.1039/c1cp22317h.

(73) MicrocalTM iTC$_{200}$ System User Manual MAN0560. Malvern 2014.
(74) Boiocchi, M.; Del Boca, L.; Gómez, D. E.; Fabbrizzi, L.; Licchelli, M.; Monzani, E. Nature of Urea-Fluoride Interaction: Incipient and Definitive Proton Transfer. *Journal of the American Chemical Society* **2004**, *126* (50), 16507–16514.
(75) Boiocchi, M.; Del Boca, L.; Esteban-Gómez, D.; Fabbrizzi, L.; Licchelli, M.; Monzani, E. Anion-Induced Urea Deprotonation. *Chemistry – A European Journal* **2005**, *11* (10), 3097–3104. https://doi.org/10.1002/chem.200401049.
(76) Wang, T.; Wang, H.-F.; Yan, X.-P. Fabrication of Anion Complexes from 5,6-Dihydrodiindolo[3,2-a:2′,3′-c]Phenazine as a Building Block. *CrystEngComm* **2010**, *12* (10), 3177. https://doi.org/10.1039/b927229a.
(77) Courtemanche, R. J. M.; Pinter, T.; Hof, F. Just Add Tetrazole: 5-(2-Pyrrolo)Tetrazoles Are Simple, Highly Potent Anion Recognition Elements. *Chemical Communications* **2011**, *47* (47), 12688. https://doi.org/10.1039/c1cc15875a.
(78) COSMOthermX Version 18 Release Notes. COSMOlogic GmbH & Co. KG March 2018.
(79) Powell, D. L.; Klaeboe, P.; Gruodis, A.; Nielsen, C. J.; Guirgis, G. A.; Durig, J. R.; Aleksa, V. Infrared and Raman Spectra, Conformations and Ab Initio Calculations of Ethyl Bromosilane and Ethyl Dibromosilane. *Journal of molecular structure* **1999**, *482*, 391–396.
(80) Guirgis, G. A.; Nashed, Y. E.; Klaeboe, P.; Durig, J. R. Conformational Stabilities, Ab Initio Calculations and Structural Parameters for 2-Chloroethyl Silane and 2-Chloroethyl Trifluorosilane. *Journal of molecular structure* **1999**, *482*, 385–389.
(81) Guirgis, G. A.; Yu, Z.; Durig, J. R. Infrared and Raman Spectra, Conformational Stability, Barrier to Internal Rotation, and Ab Initio Calculations of 1, 1-Difluoropropane. *Journal of molecular structure* **1999**, *509* (1), 307–328.
(82) Durig, J. R.; Shen, S.; Zhu, X.; Wurrey, C. J. Conformational and Structural Studies of Chloromethylcyclopropane and Bromomethylcyclopropane from Temperature Dependent FT-IR Spectra of Xenon Solutions and Ab Initio Calculations. *Journal of molecular structure* **1999**, *485*, 501–521.
(83) Cinar, M.; Karabacak, M.; Asiri, A. M. An Experimental and Density Functional Study on Conformational and Spectroscopic Analysis of 5-Methoxyindole-2-Carboxylic Acid. *Spectrochimica Acta Part A: Molecular and Biomolecular Spectroscopy* **2015**, *137*, 670–676. https://doi.org/10.1016/j.saa.2014.08.090.
(84) Szabó, A.; Kovács, A. Hydrogen Bonding and Molecular Vibrations of 2, 5-Dihydroxy-1, 4-Benzoquinone. *Journal of molecular structure* **1999**, *510* (1), 215–225.
(85) Ośmiałowski, B.; Nissinen, M.; Kolehmainen, E.; Gawinecki, R. NMR Spectral and X-Ray Structural Investigation of 1, 3-Bis (2-Quinolyl)-2-(p-Chlorophenyl)-2-Propanol. *Journal of Molecular Structure* **2000**, *525* (1), 241–245.
(86) Marlin, D. S.; Olmstead, M. M.; Mascharak, P. K. Extended Structures Controlled by Intramolecular and Intermolecular Hydrogen Bonding: A Case Study with Pyridine-2,6-Dicarboxamide, 1,3-Benzenedicarboxamide and N,N`-Dimethyl-2,6-Pyridinedicarboxamide. *Journal of Molecular Structure* **2000**, *554*, 211–223.
(87) Szady-Chełmieniecka, A.; Rozwadowski, Z.; Dziembowska, T.; Grech, E.; Wojciechowski, G.; Brzezinski, B. Intramolecular Hydrogen Bonds in 3-Diethylaminomethyl-5-R-Salicylic Aldehydes. *Journal of Molecular Structure* **2000**, *520* (1), 39–43.

(88) Beraldo, H.; Lima, R.; Teixeira, L. R.; Moura, A. A.; West, D. X. Crystal Structures and IR, NMR and UV Spectra of 4-Formyl-and 4-Acetylpyridine N (4)-Methyl-and N (4)-Ethylthiosemicarbazones. *Journal of Molecular Structure* **2001**, *559* (1), 99–106.
(89) Beraldo, H.; Lima, R.; Teixeira, L. R.; Moura, A. A.; West, D. X. Crystal Structures and IR, NMR and UV Spectra of 3-Formyl- and 3-Acetylpyridine N (4)-Methylthiosemicarbazones. *Journal of Molecular Structure* **2000**, *553*, 43–48.
(90) Prezhdo, V. V.; Ovsiankina, E. V.; Prezhdo, O. V. Conformational Analysis of Chloroalkyl Derivatives of 1,4-Naphthoquinone. *Journal of Molecular Structure* **2000**, *522*, 71–77.
(91) Pihlaja, K.; Rossi, K.; Nikander, H. Conformational Analysis. 25. 13C NMR Chemical Shifts-Sensitive Detectors in Structure Determination. 3. The Proposal for Non-Chair Conformations in Methyl-Substituted 2-Oxo-1,3,2-Dioxathianes Challenged. *The Journal of Organic Chemistry* **1985**, *50* (5), 644–649.
(92) Rampal, J. B.; Berlin, K. D.; Edasery, J. P.; Satyamurthy, N.; Van der Helm, D. Carbon-Phosphorus Heterocycles. Synthesis and Conformational Analysis of Alkyl-Substituted 1, 2, 6-Triphenyl-4-Phosphorinanones and Derivatives. *The Journal of Organic Chemistry* **1981**, *46* (6), 1166–1172.
(93) Balachander, R.; Sameera, S. A.; Mohan, R. T. S. Synthesis and 1H and 13C NMR Spectral Study of Some r(2),c(4)-Bis(Isopropylcarbonyl)-c(5)-Hydroxy-t(5)-Methyl-t(3)-Substituted Phenyl, Cyclohexanones and Their Oximes. *Journal of Molecular Structure* **2016**, *1115*, 63–69. https://doi.org/10.1016/j.molstruc.2016. 02.086.
(94) Podányi, B.; Hermecz, I.; Vasvári-Debreczy, L.; Horváth, Á. Nitrogen Bridgehead Compounds. 62. Conformational Analysis of 6,7,8,9-Tetrahydro-4H-Pyrido[1,2-a]Pyrimidin-4-Ones and Their Methyl Derivatives by NMR Spectroscopy. *The Journal of Organic Chemistry* **1986**, *51* (3), 395–399.
(95) Landis, M. E.; Mitchell, J. C.; Offen, D. L. Conformational Analysis of Fused-Ring 1, 2-Diazetidines by Carbon-13 Nuclear Magnetic Resonance Spectroscopy. *The Journal of Organic Chemistry* **1981**, *46* (3), 501–505.
(96) Pihlaja, K.; Rossi, K. Conformational Analysis. XXIII. 13C and 1H NMR Conformational Study of 2-Oxo-1,3-Dioxane and Its Methyl Derivatives. *Acta Chemica Scandinavica* **1983**, *37* (B), 289–296.
(97) Petterson, K. A.; Stein, R. S.; Drake, M. D.; Roberts, J. D. An NMR Investigation of the Importance of Intramolecular Hydrogen Bonding in Determining the Conformational Equilibrium of Ethylene Glycol in Solution. *Magn. Reson. Chem.* **2005**, *43* (3), 225–230. https://doi.org/10.1002/mrc.1512.
(98) Bürgi, T.; Baiker, A. Conformational Behavior of Cinchonidine in Different Solvents: A Combined NMR and Ab Initio Investigation. *J. Am. Chem. Soc.* **1998**, *120* (49), 12920–12926. https://doi.org/10.1021/ja982466b.
(99) Molin, W. T. Glyphosate, a Unique Global Herbicide. J. E. Franz, M. K. Mao, and J. A. Sikorski, ACS Monograph 189, 1997. 653 Pp. *Weed technol.* **1998**, *12* (3), 564–565. https://doi.org/10.1017/S0890037X0004433X.
(100) Chen, Z.; He, W.; Beer, M.; Megharaj, M.; Naidu, R. Speciation of Glyphosate, Phosphate and Aminomethylphosphonic Acid in Soil Extracts by Ion Chromatography with Inductively Coupled Plasma Mass Spectrometry with an Octopole Reaction System. *Talanta* **2009**, *78* (3), 852–856. https://doi.org/10.1016/j.talanta.2008.12.052.

(101) Sanchez, G.; Espinosa, A.; Curiel, D.; Tarraga, A.; Molina, P. Bis(Carbazolyl)Ureas as Selective Receptors for the Recognition of Hydrogenpyrophosphate in Aqueous Media. *J. Org. Chem.* **2013**, *78* (19), 9725–9737. https://doi.org/10.1021/jo401430d.
(102) Poonia, N. S.; Bajaj, A. V. Coordination Chemistry of Alkali and Alkaline Earth Cations. *Chemical Reviews* **1979**, *79* (5), 389–445. https://doi.org/10.1021/cr60321a002.
(103) Izatt, R. M.; Terry, R. E.; Haymore, B. L.; Hansen, L. D.; Dalley, N. K.; Avondet, A. G.; Christensen, J. J. Calorimetric Titration Study of the Interaction of Several Uni- and Bivalent Cations with 15-Crown-5, 18-Crown-6, and Two Isomers of Dicyclohexo-18-Crown-6 in Aqueous Solution at 25.Degree.C and .Mu. = 0.1. *Journal of the American Chemical Society* **1976**, *98* (24), 7620–7626. https://doi.org/10.1021/ja00440a028.
(104) Michaux, G.; Reisse, J. Solution Thermodynamic Studies. Part 6. Enthalpy-Entropy Compensation for the Complexation Reactions of Some Crown Ethers with Alkaline Cations: A Quantitative Interpretation of the Complexing Properties of 18-Crown-6. *Journal of the American Chemical Society* **1982**, *104* (25), 6895–6899. https://doi.org/10.1021/ja00389a002.
(105) Liu, Y.; Jing, H. A Study on Thermodynamic Properties of Crown Ether Complexation – Effect of Anions on the Complexation of 1,4,7,10,13,16-Hexaoxacyclooctadecan with Some Potassium Salts in Aqueous Solution. *Acta Physico-Chimica Sinica* **1987**, *3* (1), 11–15.
(106) Ozutsumi, K.; Ishiguro, S. A Precise Calorimetric Study of 18-Crown-6 Complexes with Sodium, Potassium, Rubidium, Caesium , and Ammonium Ions in Aqueous Solution. *Bull. Chem. Soc. Jpn.* **1992**, *65*, 1173–1175.
(107) Spencer, J. N.; Mihalick, J. E.; Nicholson, T. J.; Cortina, P. A.; Rinehimer, J. L.; Smith, J. E.; Ke, X.; He, Q.; Daniels, S. E. Comparison of the Macrocyclic Effect for Ether Hosts in Aqueous and Organic Solvents. *The Journal of Physical Chemistry* **1993**, *97* (40), 10509–10512. https://doi.org/10.1021/j100142a040.
(108) Wang, P.; Izatt, R. M.; Gillespie, S. E.; Oscarson, J. L.; Zhang, X. X.; Wang, C.; Lamb, J. D. Thermodynamics of the Interaction of 18-Crown-6 with K^+, Ti^+, Ba^{2+}, Sr^{2+} and Pb^{2+} from 323.15 to 398.15 K. *Journal of the Chemical Society, Faraday Transactions* **1995**, *91* (23), 4207. https://doi.org/10.1039/ft9959104207.
(109) Buschmann, H.-J.; Mutihac, R.-C.; Schollmeyer, E. Complex Formation of 18-Crown-6 with Metal Cations and Ammonium Ions in Dioxane–Water Mixtures. *Thermochimica Acta* **2008**, *472* (1–2), 17–19. https://doi.org/10.1016/j.tca.2008.03.010.
(110) Ràfols, C.; Bosch, E.; Barbas, R.; Prohens, R. The Ca^{2+}–EDTA Chelation as Standard Reaction to Validate Isothermal Titration Calorimeter Measurements (ITC). *Talanta* **2016**, *154*, 354–359. https://doi.org/10.1016/j.talanta.2016.03.075.
(111) Ellison, S. L. R.; Williams, A.; Eurachem Working Group on Uncertainty in Chemical Measurement. *Quantifying Uncertainty in Analytical Measurement*; Eurachem: London, 1995.
(112) Leito, I.; Helm, I. Metrology in Chemistry: Some Questions and Answers. *J.Chem.Metrol.* **2020**, *14* (2), 83–87. https://doi.org/10.25135/jcm.50.20.10.1838.

SUMMARY IN ESTONIAN

Anioonretseptorite arvutuslik disain ning peremees-külaline seondumise uurimine

Käesoleva töö esimeses osas uuriti COSMO-RS arvutusmeetodi rakendatavust anioonretseptorite disaini juures, et leida sobivaid retseptoreid analüütiliselt olulistele anioonidele (glüfosaadi dianioon ja väiksed monokarboksülaatanioonid). Töö põhirõhk keskendus seondumise steeriliste efektide vaatlemisele ning COSMO-RS meetodi kasutusala uurimisele ning meetodi rakendamises kitsaskohtade leidmisele retseptor-anioon seondumistugevuse hindamise ning anioonretseptorite arvutusliku karakteriseerimise jaoks.

Selleks, et kontrollida COSMO-RS meetodi suutlikkust lahuse keskkonnas molekulide stabiilseimaid konformeere õigesti ennustada, uuriti 105 väikest molekuli. Leiti, et üldiselt (103 juhul 105 molekulist) suudab meetod uuritud molekulide kõige stabiilsemat konformeeri õigesti ennustada.

Järgmisena uuriti väikeseid indolokarbasooli ning uurea klassidesse kuuluvaid retseptormolekule, et hinnata COSMO-RS meetodi suutlikkust korrektselt ennustada retseptor-anioon komplekside seondumistugevust. Leiti, et kuigi absoluutväärtuste poolest ei suuda meetod seondumiskonstantide väärtusi täpselt ennustada, siis seondumistugevuse trendid erinevate retseptorite ning erinevate anioonide vahel on ennustatud enam-vähem rahuldavalt.

Edasi kasutati eelnevalt uuritud väikeste retseptorite strukruuridest indooli-, karbasooli-, indolokarbasooli- ja uurea fragmente suuremate retseptormolekulide disainimiseks. Arvutuslikult uuriti nii lineaarse struktuuriga molekule (seonduvad rühmad retseptori otstes, mis on omavahel ühendatud tsüklilise või alküülse linkerrühma abil) kui ka makrotsüklilise struktuuriga molekule.

Erineva linkeri struktuuriga retseptorite disaini arvutuslikust uurimisest saab välja tuua need järeldused:

- Seotava aniooni ja vaba retseptori eelistatud geomeetria peavad üksteise jaoks sobivad olema. Siduvate rühmade asukoht ja linkerrühma pikkus ning jäikus mõjutavad anioon-retseptor kompleksi seondumistugevust, kuid nendevaheline seos ei ole lihtsalt ennustatav.
- Steerilistel efektidel on seondumistugevusele märgatav mõju. On võimalik, et just steerilise takistuse tõttu eelistab dianioon mõnede retseptoritega kompleksi moodustada vaid ühega oma anioonsetest tsentritest.
- COSMO-RS meetodit saab enamikel juhtudel rakendada eelkõige retseptorite ning nende anioonkomplekside geomeetriliste parameetrite hinnangu jaoks – eelistatud konformatsioonid, kas seonduv anioon on „piisavalt väike“ või kas retseptori sidumistasku „piisavalt suur“, kas vesiniksideme doonor- ja aktseptorrühmad on omavahel sobival kaugusel jne.
- COSMO-RS meetodit ei ole üldiselt võimalik kasutada retseptor-anioon seondumistugevuse ($\log K_{ass}$ väärtuste) hindamiseks. $\log K_{ass}$ absoluutväärtused on anioonretseptorite jaoks väga tugevalt ülehinnatud ka väga lihtsate

süsteemide korral. Keerulisemate süsteemide uurimisel ei ole mõistliku täpsusega ennustatud ka trendid logK_{ass} erinevate väärtustel omavahel võrdlemisel.

Makrotsükliliste retseptorite korral on seondumistugevus seotud makrotsükli õõnsuse suurusega, aga see ei ole ainus seondumist mõjutav faktor. Kuigi üldjoontes väikesed anioonid mahuvad väikesemate makrotsüklite sisse ning suuremad anioonid mitte, ei saa töö tulemuste kohaselt sellise struktuuriga makrotsüklilisi retseptoreid kasutada anioonide selektiivseks sidumiseks nende suuruse järgi. Kuna retseptorite struktuuris on sees painduv linkerrühm (erineva pikkusega alküülahel), siis saavad ka suuremad anioonid retseptoritega kompleksi moodustada, sest alküülahel paindub ning ei põhjusta seetõttu steerilist takistust. Töös uuritud makrotsüklilistest retseptoritest olid kõikide uuritud anioonide suhtes suurima seondumistugevusega kaks keskmise suurusega molekuli.

Töö teises osas hinnatakse väikese koguruumalaga mikrokalorimeetria rakendatavust madala seondumisafiinsusega peremees-külaline seondumisreaktsioonide uurimiseks (eelkõige reaktsioonientalpia hindamiseks). Eksperimentide kõrval on läbi viidud ka põhjalik mõõtemääramatuse hindamine, et leida selliste eksperimentide jaoks olulisemad mõõtemääramatuse komponendid ning hinnata kalorimeetriliste eksperimentide abil leitud reaktsioonientalpia väärtuste täpsust. Töö tulemusena on toodud soovitused eksperimentide planeerimiseks madala seondumisafiinsusega süsteemide uurimisel. Saadud reaktsioonientalpia hinnangu liitstandardmääramatus jääb vahemikku 1-2 kJ/mol. Suurima osakaaluga mõõtemääramatuse komponendid ITC eksperimentide juures on reaktsioonil vabaneva soojushulga mõõtmise mõõtemääramatus ning kasutatud lahuste kontsentratsioonide mõõtemääramatus.

ACKNOWLEDGEMENTS

This work has been partially supported by the Estonian Research Council grant PRG690.

This work has been partially supported by Graduate School of Functional materials and technologies receiving funding from the European Regional Development Fund in University of Tartu, Estonia.

Some of the computational results presented in this work were obtained using the High-Performance Computing Center of the University of Tartu.

I would like to express my deepest gratitude to my supervisor, Professor Ivo Leito, for the long-time support and guidance throughout my studies. I would like to thank all my work colleagues from the Chair of Analytical Chemistry and especially the co-authors of my work for the interesting discussions and wonderful work environment.

I would like to thank Lauri Sikk for all the help in technical matters related to calorimetric measurements and instrumentation and for creating the script used in the data treatment of the calorimetric measurements.

I would like to thank Ly Porosk and Tanel Tenson's group in the University of Tartu Institute of Technology for allowing me to use the MicroCal iTC_{200} microcalorimeter in the experiments carried out in this work.

I would like to thank my family, especially my husband Ian for always being supportive to me.

APPENDICES

Appendix 1. Macrocyclic receptor complexes with the acetate anion (work[IV])

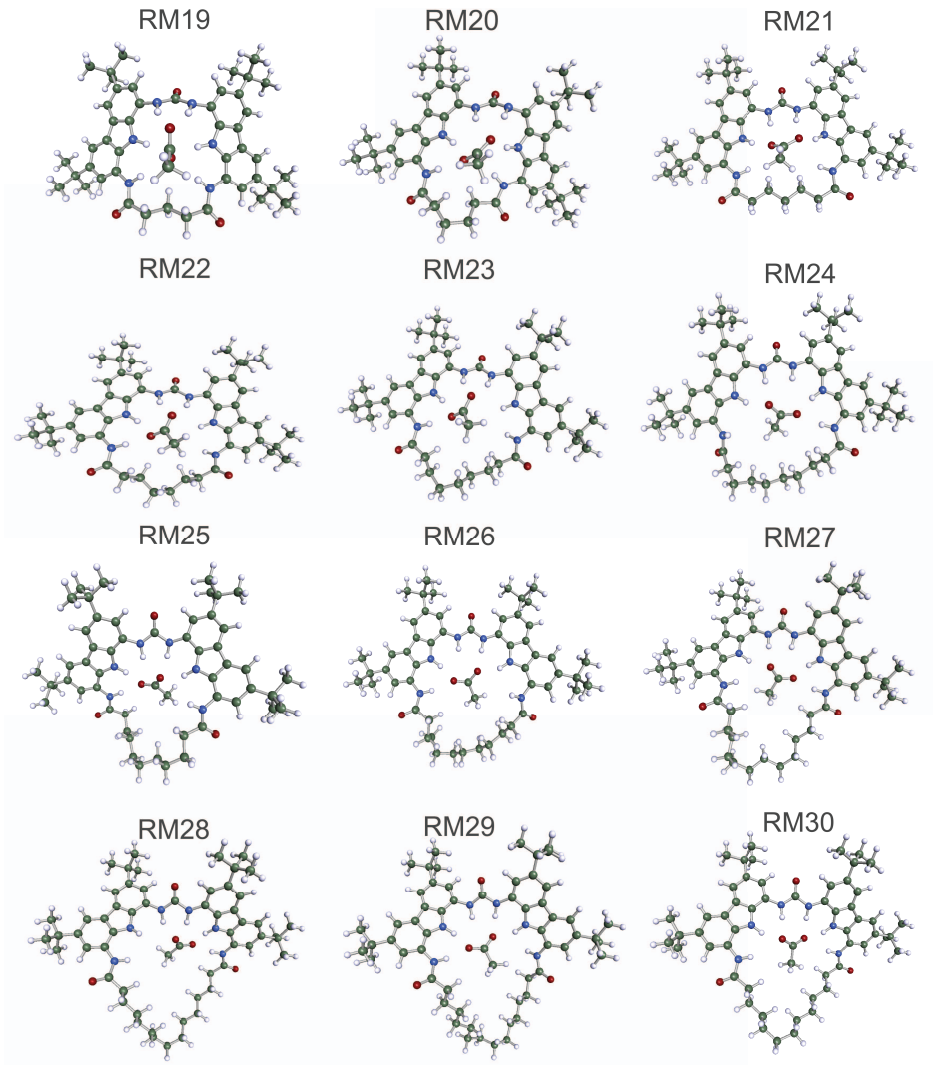

Scheme S3. Acetate complexes of macrocyclic receptors RM19-RM30.

PUBLICATIONS

CURRICULUM VITAE

Name: Astrid Darnell (née Pung)
Date of birth: March 20, 1990
Citizenship: Estonian
Contact: University of Tartu, Institute of Chemistry, Ravila 14a, Tartu, 50411, Estonia
E-mail: astrid.darnell@ut.ee
Position: Chemist (0.5)

Education:

2016–...	University of Tartu, doctoral studies (field: chemistry)
2012–2014	University of Tartu, M Sc Eng, Applied measurement science
2009–2012	University of Tartu, B Sc, chemistry

Employment:

2015–...	chemist, University of Tartu, Institute of Chemistry
2014–2015	quality specialist, Tartu Observatory, University of Tartu

Publications:

1. Darnell, A.; Sikk, L.; Porosk, L.; Leito, I. Uncertainty of small enthalpy effects measured by isothermal calorimetric titration. *Journal of Chemical Metrology* **2021**,*15, 1*. DOI: 10.25135/jcm.57.21.03.1994.
2. Tshepelevitsch, S.; Kadam, S. A.; Darnell, A.; Bobacka, J.; Rüütel, A.; Haljasorg, T.; Leito, I. LogP determination for highly lipophilic hydrogen-bonding anion receptor molecules. *Analytica Chimica Acta* **2020**, 1132 (2), 123-133. DOI: 10.1016/j.aca.2020.07.024.
3. Rüütel, A.; Yrjana, V.; Kadam, S. A.; Saar, I.; Ilisson, M.; Darnell, A.; Haav, K.; Haljasorg, T.; Toom, L.; Bobacka, J.; Leito, I. Design, synthesis and application of carbazole macrocycles in anion sensors. *Beilstein Journal of Organic Chemistry* **2020**, 16, 1901-1914. DOI: 10.3762/bjoc.16.157.
4. Kütt, A.; Selberg, S.; Kaljurand, I.; Tshepelevitsh, S.; Heering, A.; Darnell, A.; Kaupmees, K.; Piirsalu, M.; Leito, I. pKa values in organic chemistry – Making maximum use of the available data. Tetrahedron Letters **2018,** 59 (42), 3738−3748. DOI: 10.1016/j.tetlet.2018.08.054.
5. Pung, A.; Leito, I. Predicting Relative Stability of Conformers in Solution with COSMO-RS. *Journal of Physical Chemistry A* **2017**, 121 (36), 6823−6829.10.1021/acs.jpca.7b05197.
6. Martin, K.; Nõges, J.; Haav, K.; Kadam, S. A.; Pung, A.; Leito, I. Exploring Selectivity of 22 Acyclic Urea-, Carbazole- and Indolocarbazole-Based Receptors towards 11 Monocarboxylates. *European Journal of Organic Chemistry* **2017**, 35, 5231−5237.10.1002/ejoc.201700931.
7. Kadam, S. A.; Haav, K.; Toom, L.; Pung, A.; Mayeux, C.; Leito, I. Multi-dentate anion receptors for binding glyphosate dianion: structure and

affinity. European Journal of Organic Chemistry **2017**, 11, 1396−1406. 10.1002/ejoc.201601583.
8. Kadam, S. A.; Martin, K.; Haav, K.; Toom, L.; Mayeux, C.; Pung, A.; Gale, P. A.; Hiscock, J. R.; Brooks, S. J.; Kirby, I. L.; Busschaert, N.; Leito, I. Towards the Discrimination of Carboxylates by Hydrogen-Bond Donor Anion Receptors. *Chemistry – A European Journal* **2015**, 21 (13), 5145−5160.10.1002/chem.201405858.
9. Tshepelevitsh, S.; Oss, M.; Pung, A.; Leito, I. Evaluating the COSMO-RS Method for Modeling Hydrogen Bonding in Solution. *ChemPhysChem* **2013**, 14 (9), 1909−1919.10.1002/cphc.201300186.

ELULOOKIRJELDUS

Nimi: Astrid Darnell (née Pung)
Sünniaeg: 20. märts 1990
Kodakondsus: Eesti
Kontakt: Tartu Ülikooli Keemia Instituut, Ravila 14a, Tartu, 50411, Eesti
E-post: astrid.darnell@ut.ee
Töökoht: keemik, 0.5k

Hariduskäik:

2016–...	Tartu Ülikool, keemia eriala doktoriõpe
2012–2014	Tartu Ülikool, magistriõpe, rakenduslik mõõteteadus
2009–2012	Tartu Ülikool, bakalaureuseõpe, keemia

Teenistuskäik:

2015–...	keemik, Tartu Ülikool, Keemia Instituut
2014–2015	kvaliteedispetsialist, Tartu Ülikooli Tartu Observatoorium

Teaduspublikatsioonid:

1. Darnell, A.; Sikk, L.; Porosk, L.; Leito, I. Uncertainty of small enthalpy effects measured by isothermal calorimetric titration. *Journal of Chemical Metrology* **2021**,*15, 1*. DOI: 10.25135/jcm.57.21.03.1994.
2. Tshepelevitsch, S.; Kadam, S. A.; Darnell, A.; Bobacka, J.; Rüütel, A.; Haljasorg, T.; Leito, I. LogP determination for highly lipophilic hydrogen-bonding anion receptor molecules. *Analytica Chimica Acta* **2020**, 1132 (2), 123-133. DOI: 10.1016/j.aca.2020.07.024.
3. Rüütel, A.; Yrjana, V.; Kadam, S. A.; Saar, I.; Ilisson, M.; Darnell, A.; Haav, K.; Haljasorg, T.; Toom, L.; Bobacka, J.; Leito, I. Design, synthesis and application of carbazole macrocycles in anion sensors. Beilstein Journal of Organic Chemistry **2020**, 16, 1901-1914. DOI: 10.3762/bjoc.16.157.
4. Kütt, A.; Selberg, S.; Kaljurand, I.; Tshepelevitsh, S.; Heering, A.; Darnell, A.; Kaupmees, K.; Piirsalu, M.; Leito, I. pKa values in organic chemistry – Making maximum use of the available data. *Tetrahedron Letters* **2018,** 59 (42), 3738−3748. DOI: 10.1016/j.tetlet.2018.08.054.
5. Pung, A.; Leito, I. Predicting Relative Stability of Conformers in Solution with COSMO-RS. *Journal of Physical Chemistry A* **2017**, 121 (36), 6823−6829.10.1021/acs.jpca.7b05197.
6. Martin, K.; Nõges, J.; Haav, K.; Kadam, S. A.; Pung, A.; Leito, I. Exploring Selectivity of 22 Acyclic Urea-, Carbazole- and Indolocarbazole-Based Receptors towards 11 Monocarboxylates. *European Journal of Organic Chemistry* **2017**, 35, 5231−5237.10.1002/ejoc.201700931.
7. Kadam, S. A.; Haav, K.; Toom, L.; Pung, A.; Mayeux, C.; Leito, I. Multi-dentate anion receptors for binding glyphosate dianion: structure and

affinity. European Journal of Organic Chemistry **2017**, 11, 1396−1406. 10.1002/ejoc.201601583.
8. Kadam, S. A.; Martin, K.; Haav, K.; Toom, L.; Mayeux, C.; Pung, A.; Gale, P. A.; Hiscock, J. R.; Brooks, S. J.; Kirby, I. L.; Busschaert, N.; Leito, I. Towards the Discrimination of Carboxylates by Hydrogen-Bond Donor Anion Receptors. *Chemistry – A European Journal* **2015**, 21 (13), 5145−5160.10.1002/chem.201405858.
9. Tshepelevitsh, S.; Oss, M.; Pung, A.; Leito, I. Evaluating the COSMO-RS Method for Modeling Hydrogen Bonding in Solution. *ChemPhysChem* **2013**, 14 (9), 1909−1919.10.1002/cphc.201300186.

DISSERTATIONES CHIMICAE UNIVERSITATIS TARTUENSIS

1. **Toomas Tamm.** Quantum-chemical simulation of solvent effects. Tartu, 1993, 110 p.
2. **Peeter Burk.** Theoretical study of gas-phase acid-base equilibria. Tartu, 1994, 96 p.
3. **Victor Lobanov.** Quantitative structure-property relationships in large descriptor spaces. Tartu, 1995, 135 p.
4. **Vahur Mäemets.** The ^{17}O and ^{1}H nuclear magnetic resonance study of H_2O in individual solvents and its charged clusters in aqueous solutions of electrolytes. Tartu, 1997, 140 p.
5. **Andrus Metsala.** Microcanonical rate constant in nonequilibrium distribution of vibrational energy and in restricted intramolecular vibrational energy redistribution on the basis of slater's theory of unimolecular reactions. Tartu, 1997, 150 p.
6. **Uko Maran.** Quantum-mechanical study of potential energy surfaces in different environments. Tartu, 1997, 137 p.
7. **Alar Jänes.** Adsorption of organic compounds on antimony, bismuth and cadmium electrodes. Tartu, 1998, 219 p.
8. **Kaido Tammeveski.** Oxygen electroreduction on thin platinum films and the electrochemical detection of superoxide anion. Tartu, 1998, 139 p.
9. **Ivo Leito.** Studies of Brønsted acid-base equilibria in water and non-aqueous media. Tartu, 1998, 101 p.
10. **Jaan Leis.** Conformational dynamics and equilibria in amides. Tartu, 1998, 131 p.
11. **Toonika Rinken.** The modelling of amperometric biosensors based on oxidoreductases. Tartu, 2000, 108 p.
12. **Dmitri Panov.** Partially solvated Grignard reagents. Tartu, 2000, 64 p.
13. **Kaja Orupõld.** Treatment and analysis of phenolic wastewater with microorganisms. Tartu, 2000, 123 p.
14. **Jüri Ivask.** Ion Chromatographic determination of major anions and cations in polar ice core. Tartu, 2000, 85 p.
15. **Lauri Vares.** Stereoselective Synthesis of Tetrahydrofuran and Tetrahydropyran Derivatives by Use of Asymmetric Horner-Wadsworth-Emmons and Ring Closure Reactions. Tartu, 2000, 184 p.
16. **Martin Lepiku.** Kinetic aspects of dopamine D_2 receptor interactions with specific ligands. Tartu, 2000, 81 p.
17. **Katrin Sak.** Some aspects of ligand specificity of P2Y receptors. Tartu, 2000, 106 p.
18. **Vello Pällin.** The role of solvation in the formation of iotsitch complexes. Tartu, 2001, 95 p.
19. **Katrin Kollist.** Interactions between polycyclic aromatic compounds and humic substances. Tartu, 2001, 93 p.

20. **Ivar Koppel.** Quantum chemical study of acidity of strong and superstrong Brønsted acids. Tartu, 2001, 104 p.
21. **Viljar Pihl.** The study of the substituent and solvent effects on the acidity of OH and CH acids. Tartu, 2001, 132 p.
22. **Natalia Palm.** Specification of the minimum, sufficient and significant set of descriptors for general description of solvent effects. Tartu, 2001, 134 p.
23. **Sulev Sild.** QSPR/QSAR approaches for complex molecular systems. Tartu, 2001, 134 p.
24. **Ruslan Petrukhin.** Industrial applications of the quantitative structure-property relationships. Tartu, 2001, 162 p.
25. **Boris V. Rogovoy.** Synthesis of (benzotriazolyl)carboximidamides and their application in relations with *N*- and *S*-nucleophyles. Tartu, 2002, 84 p.
26. **Koit Herodes.** Solvent effects on UV-vis absorption spectra of some solvatochromic substances in binary solvent mixtures: the preferential solvation model. Tartu, 2002, 102 p.
27. **Anti Perkson.** Synthesis and characterisation of nanostructured carbon. Tartu, 2002, 152 p.
28. **Ivari Kaljurand.** Self-consistent acidity scales of neutral and cationic Brønsted acids in acetonitrile and tetrahydrofuran. Tartu, 2003, 108 p.
29. **Karmen Lust.** Adsorption of anions on bismuth single crystal electrodes. Tartu, 2003, 128 p.
30. **Mare Piirsalu.** Substituent, temperature and solvent effects on the alkaline hydrolysis of substituted phenyl and alkyl esters of benzoic acid. Tartu, 2003, 156 p.
31. **Meeri Sassian.** Reactions of partially solvated Grignard reagents. Tartu, 2003, 78 p.
32. **Tarmo Tamm.** Quantum chemical modelling of polypyrrole. Tartu, 2003. 100 p.
33. **Erik Teinemaa.** The environmental fate of the particulate matter and organic pollutants from an oil shale power plant. Tartu, 2003. 102 p.
34. **Jaana Tammiku-Taul.** Quantum chemical study of the properties of Grignard reagents. Tartu, 2003. 120 p.
35. **Andre Lomaka.** Biomedical applications of predictive computational chemistry. Tartu, 2003. 132 p.
36. **Kostyantyn Kirichenko.** Benzotriazole – Mediated Carbon–Carbon Bond Formation. Tartu, 2003. 132 p.
37. **Gunnar Nurk.** Adsorption kinetics of some organic compounds on bismuth single crystal electrodes. Tartu, 2003, 170 p.
38. **Mati Arulepp.** Electrochemical characteristics of porous carbon materials and electrical double layer capacitors. Tartu, 2003, 196 p.
39. **Dan Cornel Fara.** QSPR modeling of complexation and distribution of organic compounds. Tartu, 2004, 126 p.
40. **Riina Mahlapuu.** Signalling of galanin and amyloid precursor protein through adenylate cyclase. Tartu, 2004, 124 p.

41. **Mihkel Kerikmäe.** Some luminescent materials for dosimetric applications and physical research. Tartu, 2004, 143 p.
42. **Jaanus Kruusma.** Determination of some important trace metal ions in human blood. Tartu, 2004, 115 p.
43. **Urmas Johanson.** Investigations of the electrochemical properties of polypyrrole modified electrodes. Tartu, 2004, 91 p.
44. **Kaido Sillar.** Computational study of the acid sites in zeolite ZSM-5. Tartu, 2004, 80 p.
45. **Aldo Oras.** Kinetic aspects of dATPαS interaction with $P2Y_1$ receptor. Tartu, 2004, 75 p.
46. **Erik Mölder.** Measurement of the oxygen mass transfer through the air-water interface. Tartu, 2005, 73 p.
47. **Thomas Thomberg.** The kinetics of electroreduction of peroxodisulfate anion on cadmium (0001) single crystal electrode. Tartu, 2005, 95 p.
48. **Olavi Loog.** Aspects of condensations of carbonyl compounds and their imine analogues. Tartu, 2005, 83 p.
49. **Siim Salmar.** Effect of ultrasound on ester hydrolysis in aqueous ethanol. Tartu, 2006, 73 p.
50. **Ain Uustare.** Modulation of signal transduction of heptahelical receptors by other receptors and G proteins. Tartu, 2006, 121 p.
51. **Sergei Yurchenko.** Determination of some carcinogenic contaminants in food. Tartu, 2006, 143 p.
52. **Kaido Tämm.** QSPR modeling of some properties of organic compounds. Tartu, 2006, 67 p.
53. **Olga Tšubrik.** New methods in the synthesis of multisubstituted hydrazines. Tartu. 2006, 183 p.
54. **Lilli Sooväli.** Spectrophotometric measurements and their uncertainty in chemical analysis and dissociation constant measurements. Tartu, 2006, 125 p.
55. **Eve Koort.** Uncertainty estimation of potentiometrically measured ph and pK_a values. Tartu, 2006, 139 p.
56. **Sergei Kopanchuk.** Regulation of ligand binding to melanocortin receptor subtypes. Tartu, 2006, 119 p.
57. **Silvar Kallip.** Surface structure of some bismuth and antimony single crystal electrodes. Tartu, 2006, 107 p.
58. **Kristjan Saal.** Surface silanization and its application in biomolecule coupling. Tartu, 2006, 77 p.
59. **Tanel Tätte.** High viscosity $Sn(OBu)_4$ oligomeric concentrates and their applications in technology. Tartu, 2006, 91 p.
60. **Dimitar Atanasov Dobchev**. Robust QSAR methods for the prediction of properties from molecular structure. Tartu, 2006, 118 p.
61. **Hannes Hagu**. Impact of ultrasound on hydrophobic interactions in solutions. Tartu, 2007, 81 p.
62. **Rutha Jäger.** Electroreduction of peroxodisulfate anion on bismuth electrodes. Tartu, 2007, 142 p.

63. **Kaido Viht.** Immobilizable bisubstrate-analogue inhibitors of basophilic protein kinases: development and application in biosensors. Tartu, 2007, 88 p.
64. **Eva-Ingrid Rõõm.** Acid-base equilibria in nonpolar media. Tartu, 2007, 156 p.
65. **Sven Tamp.** DFT study of the cesium cation containing complexes relevant to the cesium cation binding by the humic acids. Tartu, 2007, 102 p.
66. **Jaak Nerut.** Electroreduction of hexacyanoferrate(III) anion on Cadmium (0001) single crystal electrode. Tartu, 2007, 180 p.
67. **Lauri Jalukse.** Measurement uncertainty estimation in amperometric dissolved oxygen concentration measurement. Tartu, 2007, 112 p.
68. **Aime Lust.** Charge state of dopants and ordered clusters formation in CaF_2:Mn and CaF_2:Eu luminophors. Tartu, 2007, 100 p.
69. **Iiris Kahn**. Quantitative Structure-Activity Relationships of environmentally relevant properties. Tartu, 2007, 98 p.
70. **Mari Reinik.** Nitrates, nitrites, N-nitrosamines and polycyclic aromatic hydrocarbons in food: analytical methods, occurrence and dietary intake. Tartu, 2007, 172 p.
71. **Heili Kasuk.** Thermodynamic parameters and adsorption kinetics of organic compounds forming the compact adsorption layer at Bi single crystal electrodes. Tartu, 2007, 212 p.
72. **Erki Enkvist.** Synthesis of adenosine-peptide conjugates for biological applications. Tartu, 2007, 114 p.
73. **Svetoslav Hristov Slavov**. Biomedical applications of the QSAR approach. Tartu, 2007, 146 p.
74. **Eneli Härk.** Electroreduction of complex cations on electrochemically polished Bi(*hkl*) single crystal electrodes. Tartu, 2008, 158 p.
75. **Priit Möller.** Electrochemical characteristics of some cathodes for medium temperature solid oxide fuel cells, synthesized by solid state reaction technique. Tartu, 2008, 90 p.
76. **Signe Viggor.** Impact of biochemical parameters of genetically different pseudomonads at the degradation of phenolic compounds. Tartu, 2008, 122 p.
77. **Ave Sarapuu.** Electrochemical reduction of oxygen on quinone-modified carbon electrodes and on thin films of platinum and gold. Tartu, 2008, 134 p.
78. **Agnes Kütt.** Studies of acid-base equilibria in non-aqueous media. Tartu, 2008, 198 p.
79. **Rouvim Kadis.** Evaluation of measurement uncertainty in analytical chemistry: related concepts and some points of misinterpretation. Tartu, 2008, 118 p.
80. **Valter Reedo.** Elaboration of IVB group metal oxide structures and their possible applications. Tartu, 2008, 98 p.
81. **Aleksei Kuznetsov.** Allosteric effects in reactions catalyzed by the cAMP-dependent protein kinase catalytic subunit. Tartu, 2009, 133 p.

82. **Aleksei Bredihhin.** Use of mono- and polyanions in the synthesis of multisubstituted hydrazine derivatives. Tartu, 2009, 105 p.
83. **Anu Ploom.** Quantitative structure-reactivity analysis in organosilicon chemistry. Tartu, 2009, 99 p.
84. **Argo Vonk.** Determination of adenosine A_{2A}- and dopamine D_1 receptor-specific modulation of adenylate cyclase activity in rat striatum. Tartu, 2009, 129 p.
85. **Indrek Kivi.** Synthesis and electrochemical characterization of porous cathode materials for intermediate temperature solid oxide fuel cells. Tartu, 2009, 177 p.
86. **Jaanus Eskusson.** Synthesis and characterisation of diamond-like carbon thin films prepared by pulsed laser deposition method. Tartu, 2009, 117 p.
87. **Marko Lätt.** Carbide derived microporous carbon and electrical double layer capacitors. Tartu, 2009, 107 p.
88. **Vladimir Stepanov.** Slow conformational changes in dopamine transporter interaction with its ligands. Tartu, 2009, 103 p.
89. **Aleksander Trummal.** Computational Study of Structural and Solvent Effects on Acidities of Some Brønsted Acids. Tartu, 2009, 103 p.
90. **Eerold Vellemäe.** Applications of mischmetal in organic synthesis. Tartu, 2009, 93 p.
91. **Sven Parkel.** Ligand binding to 5-HT_{1A} receptors and its regulation by Mg^{2+} and Mn^{2+}. Tartu, 2010, 99 p.
92. **Signe Vahur.** Expanding the possibilities of ATR-FT-IR spectroscopy in determination of inorganic pigments. Tartu, 2010, 184 p.
93. **Tavo Romann**. Preparation and surface modification of bismuth thin film, porous, and microelectrodes. Tartu, 2010, 155 p.
94. **Nadežda Aleksejeva.** Electrocatalytic reduction of oxygen on carbon nanotube-based nanocomposite materials. Tartu, 2010, 147 p.
95. **Marko Kullapere.** Electrochemical properties of glassy carbon, nickel and gold electrodes modified with aryl groups. Tartu, 2010, 233 p.
96. **Liis Siinor.** Adsorption kinetics of ions at Bi single crystal planes from aqueous electrolyte solutions and room-temperature ionic liquids. Tartu, 2010, 101 p.
97. **Angela Vaasa.** Development of fluorescence-based kinetic and binding assays for characterization of protein kinases and their inhibitors. Tartu 2010, 101 p.
98. **Indrek Tulp.** Multivariate analysis of chemical and biological properties. Tartu 2010, 105 p.
99. **Aare Selberg.** Evaluation of environmental quality in Northern Estonia by the analysis of leachate. Tartu 2010, 117 p.
100. **Darja Lavõgina.** Development of protein kinase inhibitors based on adenosine analogue-oligoarginine conjugates. Tartu 2010, 248 p.
101. **Laura Herm.** Biochemistry of dopamine D_2 receptors and its association with motivated behaviour. Tartu 2010, 156 p.

102. **Terje Raudsepp.** Influence of dopant anions on the electrochemical properties of polypyrrole films. Tartu 2010, 112 p.
103. **Margus Marandi.** Electroformation of Polypyrrole Films: *In-situ* AFM and STM Study. Tartu 2011, 116 p.
104. **Kairi Kivirand.** Diamine oxidase-based biosensors: construction and working principles. Tartu, 2011, 140 p.
105. **Anneli Kruve.** Matrix effects in liquid-chromatography electrospray mass-spectrometry. Tartu, 2011, 156 p.
106. **Gary Urb.** Assessment of environmental impact of oil shale fly ash from PF and CFB combustion. Tartu, 2011, 108 p.
107. **Nikita Oskolkov.** A novel strategy for peptide-mediated cellular delivery and induction of endosomal escape. Tartu, 2011, 106 p.
108. **Dana Martin.** The QSPR/QSAR approach for the prediction of properties of fullerene derivatives. Tartu, 2011, 98 p.
109. **Säde Viirlaid.** Novel glutathione analogues and their antioxidant activity. Tartu, 2011, 106 p.
110. **Ülis Sõukand.** Simultaneous adsorption of Cd^{2+}, Ni^{2+}, and Pb^{2+} on peat. Tartu, 2011, 124 p.
111. **Lauri Lipping.** The acidity of strong and superstrong Brønsted acids, an outreach for the "limits of growth": a quantum chemical study. Tartu, 2011, 124 p.
112. **Heisi Kurig.** Electrical double-layer capacitors based on ionic liquids as electrolytes. Tartu, 2011, 146 p.
113. **Marje Kasari.** Bisubstrate luminescent probes, optical sensors and affinity adsorbents for measurement of active protein kinases in biological samples. Tartu, 2012, 126 p.
114. **Kalev Takkis.** Virtual screening of chemical databases for bioactive molecules. Tartu, 2012, 122 p.
115. **Ksenija Kisseljova**. Synthesis of aza-β^3-amino acid containing peptides and kinetic study of their phosphorylation by protein kinase A. Tartu, 2012, 104 p.
116. **Riin Rebane.** Advanced method development strategy for derivatization LC/ESI/MS. Tartu, 2012, 184 p.
117. **Vladislav Ivaništšev.** Double layer structure and adsorption kinetics of ions at metal electrodes in room temperature ionic liquids. Tartu, 2012, 128 p.
118. **Irja Helm.** High accuracy gravimetric Winkler method for determination of dissolved oxygen. Tartu, 2012, 139 p.
119. **Karin Kipper.** Fluoroalcohols as Components of LC-ESI-MS Eluents: Usage and Applications. Tartu, 2012, 164 p.
120. **Arno Ratas.** Energy storage and transfer in dosimetric luminescent materials. Tartu, 2012, 163 p.
121. **Reet Reinart-Okugbeni**. Assay systems for characterisation of subtype-selective binding and functional activity of ligands on dopamine receptors. Tartu, 2012, 159 p.

122. **Lauri Sikk.** Computational study of the Sonogashira cross-coupling reaction. Tartu, 2012, 81 p.
123. **Karita Raudkivi.** Neurochemical studies on inter-individual differences in affect-related behaviour of the laboratory rat. Tartu, 2012, 161 p.
124. **Indrek Saar.** Design of GalR2 subtype specific ligands: their role in depression-like behavior and feeding regulation. Tartu, 2013, 126 p.
125. **Ann Laheäär.** Electrochemical characterization of alkali metal salt based non-aqueous electrolytes for supercapacitors. Tartu, 2013, 127 p.
126. **Kerli Tõnurist.** Influence of electrospun separator materials properties on electrochemical performance of electrical double-layer capacitors. Tartu, 2013, 147 p.
127. **Kaija Põhako-Esko.** Novel organic and inorganic ionogels: preparation and characterization. Tartu, 2013, 124 p.
128. **Ivar Kruusenberg.** Electroreduction of oxygen on carbon nanomaterial-based catalysts. Tartu, 2013, 191 p.
129. **Sander Piiskop.** Kinetic effects of ultrasound in aqueous acetonitrile solutions. Tartu, 2013, 95 p.
130. **Ilona Faustova**. Regulatory role of L-type pyruvate kinase N-terminal domain. Tartu, 2013, 109 p.
131. **Kadi Tamm.** Synthesis and characterization of the micro-mesoporous anode materials and testing of the medium temperature solid oxide fuel cell single cells. Tartu, 2013, 138 p.
132. **Iva Bozhidarova Stoyanova-Slavova.** Validation of QSAR/QSPR for regulatory purposes. Tartu, 2013, 109 p.
133. **Vitali Grozovski**. Adsorption of organic molecules at single crystal electrodes studied by *in situ* STM method. Tartu, 2014, 146 p.
134. **Santa Veikšina**. Development of assay systems for characterisation of ligand binding properties to melanocortin 4 receptors. Tartu, 2014, 151 p.
135. **Jüri Liiv.** PVDF (polyvinylidene difluoride) as material for active element of twisting-ball displays. Tartu, 2014, 111 p.
136. **Kersti Vaarmets.** Electrochemical and physical characterization of pristine and activated molybdenum carbide-derived carbon electrodes for the oxygen electroreduction reaction. Tartu, 2014, 131 p.
137. **Lauri Tõntson**. Regulation of G-protein subtypes by receptors, guanine nucleotides and Mn^{2+}. Tartu, 2014, 105 p.
138. **Aiko Adamson.** Properties of amine-boranes and phosphorus analogues in the gas phase. Tartu, 2014, 78 p.
139. **Elo Kibena**. Electrochemical grafting of glassy carbon, gold, highly oriented pyrolytic graphite and chemical vapour deposition-grown graphene electrodes by diazonium reduction method. Tartu, 2014, 184 p.
140. **Teemu Näykki.** Novel Tools for Water Quality Monitoring – From Field to Laboratory. Tartu, 2014, 202 p.
141. **Karl Kaupmees.** Acidity and basicity in non-aqueous media: importance of solvent properties and purity. Tartu, 2014, 128 p.

142. **Oleg Lebedev**. Hydrazine polyanions: different strategies in the synthesis of heterocycles. Tartu, 2015, 118 p.
143. **Geven Piir.** Environmental risk assessment of chemicals using QSAR methods. Tartu, 2015, 123 p.
144. **Olga Mazina.** Development and application of the biosensor assay for measurements of cyclic adenosine monophosphate in studies of G protein-coupled receptor signalinga. Tartu, 2015, 116 p.
145. **Sandip Ashokrao Kadam.** Anion receptors: synthesis and accurate binding measurements. Tartu, 2015, 116 p.
146. **Indrek Tallo.** Synthesis and characterization of new micro-mesoporous carbide derived carbon materials for high energy and power density electrical double layer capacitors. Tartu, 2015, 148 p.
147. **Heiki Erikson.** Electrochemical reduction of oxygen on nanostructured palladium and gold catalysts. Tartu, 2015, 204 p.
148. **Erik Anderson.** *In situ* Scanning Tunnelling Microscopy studies of the interfacial structure between Bi(111) electrode and a room temperature ionic liquid. Tartu, 2015, 118 p.
149. **Girinath G. Pillai.** Computational Modelling of Diverse Chemical, Biochemical and Biomedical Properties. Tartu, 2015, 140 p.
150. **Piret Pikma.** Interfacial structure and adsorption of organic compounds at Cd(0001) and Sb(111) electrodes from ionic liquid and aqueous electrolytes: an *in situ* STM study. Tartu, 2015, 126 p.
151. **Ganesh babu Manoharan.** Combining chemical and genetic approaches for photoluminescence assays of protein kinases. Tartu, 2016, 126 p.
152. **Carolin Siimenson**. Electrochemical characterization of halide ion adsorption from liquid mixtures at Bi(111) and pyrolytic graphite electrode surface. Tartu, 2016, 110 p.
153. **Asko Laaniste.** Comparison and optimisation of novel mass spectrometry ionisation sources. Tartu, 2016, 156 p.
154. **Hanno Evard.** Estimating limit of detection for mass spectrometric analysis methods. Tartu, 2016, 224 p.
155. **Kadri Ligi.** Characterization and application of protein kinase-responsive organic probes with triplet-singlet energy transfer. Tartu, 2016, 122 p.
156. **Margarita Kagan.** Biosensing penicillins' residues in milk flows. Tartu, 2016, 130 p.
157. **Marie Kriisa.** Development of protein kinase-responsive photoluminescent probes and cellular regulators of protein phosphorylation. Tartu, 2016, 106 p.
158. **Mihkel Vestli.** Ultrasonic spray pyrolysis deposited electrolyte layers for intermediate temperature solid oxide fuel cells. Tartu, 2016, 156 p.
159. **Silver Sepp**. Influence of porosity of the carbide-derived carbon on the properties of the composite electrocatalysts and characteristics of polymer electrolyte fuel cells. Tartu, 2016, 137 p.
160. **Kristjan Haav**. Quantitative relative equilibrium constant measurements in supramolecular chemistry. Tartu, 2017, 158 p.

161. **Anu Teearu**. Development of MALDI-FT-ICR-MS methodology for the analysis of resinous materials. Tartu, 2017, 205 p.
162. **Taavi Ivan**. Bifunctional inhibitors and photoluminescent probes for studies on protein complexes. Tartu, 2017, 140 p.
163. **Maarja-Liisa Oldekop**. Characterization of amino acid derivatization reagents for LC-MS analysis. Tartu, 2017, 147 p.
164. **Kristel Jukk**. Electrochemical reduction of oxygen on platinum- and palladium-based nanocatalysts. Tartu, 2017, 250 p.
165. **Siim Kukk**. Kinetic aspects of interaction between dopamine transporter and *N*-substituted nortropane derivatives. Tartu, 2017, 107 p.
166. **Birgit Viira**. Design and modelling in early drug development in targeting HIV-1 reverse transcriptase and Malaria. Tartu, 2017, 172 p.
167. **Rait Kivi**. Allostery in cAMP dependent protein kinase catalytic subunit. Tartu, 2017, 115 p.
168. **Agnes Heering**. Experimental realization and applications of the unified acidity scale. Tartu, 2017, 123 p.
169. **Delia Juronen**. Biosensing system for the rapid multiplex detection of mastitis-causing pathogens in milk. Tartu, 2018, 85 p.
170. **Hedi Rahnel.** ARC-inhibitors: from reliable biochemical assays to regulators of physiology of cells. Tartu, 2018, 176 p.
171. **Anton Ruzanov.** Computational investigation of the electrical double layer at metal–aqueous solution and metal–ionic liquid interfaces. Tartu, 2018, 129 p.
172. **Katrin Kestav.** Crystal Structure-Guided Development of Bisubstrate-Analogue Inhibitors of Mitotic Protein Kinase Haspin. Tartu, 2018, 166 p.
173. **Mihkel Ilisson.** Synthesis of novel heterocyclic hydrazine derivatives and their conjugates. Tartu, 2018, 101 p.
174. **Anni Allikalt.** Development of assay systems for studying ligand binding to dopamine receptors. Tartu, 2018, 160 p.
175. **Ove Oll.** Electrical double layer structure and energy storage characteristics of ionic liquid based capacitors. Tartu, 2018, 187 p.
176. **Rasmus Palm.** Carbon materials for energy storage applications. Tartu, 2018, 114 p.
177. **Jörgen Metsik.** Preparation and stability of poly(3,4-ethylenedioxythiophene) thin films for transparent electrode applications. Tartu, 2018, 111 p.
178. **Sofja Tšepelevitš.** Experimental studies and modeling of solute-solvent interactions. Tartu, 2018, 109 p.
179. **Märt Lõkov.** Basicity of some nitrogen, phosphorus and carbon bases in acetonitrile. Tartu, 2018, 104 p.
180. **Anton Mastitski**. Preparation of α-aza-amino acid precursors and related compounds by novel methods of reductive one-pot alkylation and direct alkylation. Tartu, 2018, 155 p.
181. **Jürgen Vahter**. Development of bisubstrate inhibitors for protein kinase CK2. Tartu, 2019, 186 p.

182. **Piia Liigand.** Expanding and improving methodology and applications of ionization efficiency measurements. Tartu, 2019, 189 p.
183. **Sigrid Selberg.** Synthesis and properties of lipophilic phosphazene-based indicator molecules. Tartu, 2019, 74 p.
184. **Jaanus Liigand.** Standard substance free quantification for LC/ESI/MS analysis based on the predicted ionization efficiencies. Tartu, 2019, 254 p.
185. **Marek Mooste.** Surface and electrochemical characterisation of aryl film and nanocomposite material modified carbon and metal-based electrodes. Tartu, 2019, 304 p.
186. **Mare Oja.** Experimental investigation and modelling of pH profiles for effective membrane permeability of drug substances. Tartu, 2019, 306 p.
187. **Sajid Hussain.** Electrochemical reduction of oxygen on supported Pt catalysts. Tartu, 2019, 220 p.
188. **Ronald Väli.** Glucose-derived hard carbon electrode materials for sodium-ion batteries. Tartu, 2019, 180 p.
189. **Ester Tee.** Analysis and development of selective synthesis methods of hierarchical micro- and mesoporous carbons. Tartu, 2019, 210 p.
190. **Martin Maide.** Influence of the microstructure and chemical composition of the fuel electrode on the electrochemical performance of reversible solid oxide fuel cell. Tartu, 2020, 144 p.
191. **Edith Viirlaid.** Biosensing Pesticides in Water Samples. Tartu, 2020, 102 p.
192. **Maike Käärik.** Nanoporous carbon: the controlled nanostructure, and structure-property relationships. Tartu, 2020, 162 p.
193. **Artur Gornischeff.** Study of ionization efficiencies for derivatized compounds in LC/ESI/MS and their application for targeted analysis. Tartu, 2020, 124 p.
194. **Reet Link.** Ligand binding, allosteric modulation and constitutive activity of melanocortin-4 receptors. Tartu, 2020, 108 p.
195. **Pilleriin Peets.** Development of instrumental methods for the analysis of textile fibres and dyes. Tartu, 2020, 150 p.
196. **Larisa Ivanova.** Design of active compounds against neurodegenerative diseases. Tartu, 2020, 152 p.
197. **Meelis Härmas.** Impact of activated carbon microstructure and porosity on electrochemical performance of electrical double-layer capacitors. Tartu, 2020, 122 p.
198. **Ruta Hecht.** Novel Eluent Additives for LC-MS Based Bioanalytical Methods. Tartu, 2020, 202 p.
199. **Max Hecht.** Advances in the Development of a Point-of-Care Mass Spectrometer Test. Tartu, 2020, 168 p.
200. **Ida Rahu.** Bromine formation in inorganic bromide/nitrate mixtures and its application for oxidative aromatic bromination. Tartu, 2020, 116 p.
201. **Sander Ratso**. Electrocatalysis of oxygen reduction on non-precious metal catalysts. Tartu, 2020, 371 p.